

Extraction Slits for First-Order STIS Spectra

Claus Leitherer and Ralph Bohlin
September 1997

ABSTRACT:

Measurements of enclosed energy vs. extraction slit height and numerical simulations for first-order STIS spectra demonstrate the dependence of signal-to-noise (S/N) on the extraction slit height for different gratings, wavelengths, and signal levels. Slit heights of 11 pixels for G140L and G230L, and 7 pixels for the three CCD first-order modes are a reasonable compromise between photometric precision, achieved S/N, and spectral purity at most wavelengths. We recommend the implementation of these extraction slits for the pipeline and the default absolute flux calibration of archival STIS spectra of point sources.

1. Introduction

The first generation of HST spectrographs used 1-dimensional detectors: each FOS or GHRS diode recorded the entire signal within the entrance aperture along the spatial direction. Observers using the FOS and GHRS could obtain 1-dimensional spectra of their targets without having to worry about details of the light distribution along the cross-dispersion direction.

STIS is a 2-dimensional spectrograph. Information on the spatial structure of the target perpendicular to the dispersion direction is recorded on the detector and can be extracted with suitable software. Even in the case of a point source, an optimal extraction is not trivial (Horne 1986; Kinney, Bohlin, & Neill 1991). This Instrument Science Report discusses the trade-offs among different considerations and recommends the artificial slit heights for implementation in the CALSTIS simple algorithm.

2. Observations and Data Reduction

There is no optimal extraction algorithm that could satisfy every observer's needs. Even for a point source, the optimal height of an extraction aperture depends on the PSF width, the target flux relative to the background, and the trade-off between flux conserva-

tion, maximum signal-to-noise, and spectral purity. Complicated algorithms using an extraction weighted by S/N can improve the S/N of the extracted spectrum in some cases. However, a simple, robust extraction algorithm with few parameters is adequate for the scientific analysis of most point source data. For the lowest S/N data, the user may prefer to extract spectra with an algorithm of her own.

The data that define the PSF of the light perpendicular to the dispersion direction were part of SMOV proposals 7064 and 7094. Observational details are in Table 1. The PSF for other stars observed at different epochs are similar; however, a full study of the effects of breathing, jitter, and the general repeatability of the PSF is needed at all scales from the core to the wings. Our model for the S/N in simple extractions predicts the S/N as a function of slit height, target/background flux ratio, grating, and wavelength.

Table 1. Observation details

Proposal	Observation Set	Star	Grating	Central Wavelength
7064	o3yx11oym	GRW+70°5824	G140L	1425
7064	o3yx11p2m	GRW+70°5824	G230L	2376
7094	o3wy02020	BD+75°325	G230LB	2375
7094	o3wy02030	BD+75°325	G430L	4300
7094	o3wy02040	BD+75°325	G750L	7751

After the spectral images are processed through the flat fielding step, the distribution of signal is examined along the direction perpendicular to the dispersion. In particular, the images are averaged over 100 pixels along the dispersion direction, centered on pixel number 100, 300, 500, 700, 900, 975. (The window centered on pixel 975 has a size of only 50 pixels, instead of 100). The background level on the detector is defined by a 5 pixel window at a distance of 300 pixels above and below the spectrum. This background is subtracted to obtain a relative PSF, which is then normalized to unity at the center. Cross-sections of these averaged, background subtracted PSFs at the center pixels 100, 300, 500, 700, 900, and 975 are shown in Figures 1a through e for gratings G140L, G230L, G230LB, G430L, and G750L, respectively. The extended faint wings at the longest wavelengths in Figure 1e are due to scattering of light within the CCD.

3. S/N versus slit height

The S/N should initially increase with slit height, as more target flux is extracted. After a critical height is reached, S/N decreases, as more and more noise from the background is added. A slit height equal to the critical, turn-over point maximizes the S/N. Since the location of the turn-over depends on the target signal relative to the background, we simu-

lated four cases: peak signals in the center pixel above the background by factors of ∞ , 10, 5, and 2, respectively. For comparison, a V=18 mag A1V star has a peak count rate with the G230L grating at 2650 Å that is a factor of 10 above the background. Therefore, except for the case of no background at all, the chosen cases refer to observations of rather faint objects. In general, the turn-over of the S/N lies at short slit heights for cases with relatively high background levels.

The results for the case of no background are in Figures 2a through e for the five low dispersion gratings. Each figure shows the cumulative S/N, normalized to the peak S/N for each wavelength. The behavior of the curves is trivial: increasing the slit height means extracting more flux so that the S/N rises asymptotically until a finite value is reached.

The case of a peak signal 10 times the background is more interesting. The results are in Figures 3a through e, which show the cumulative S/N, normalized to the peak S/N for each wavelength. For grating G140L, the S/N increases to a slit height of at least 10 pixels and then turns over for all but the shortest wavelength. The different behavior of the 1183 Å curve results from the more extended PSF at the shortest wavelength (see the outermost envelope in Figure 1a, which is the PSF at 1183 Å). In this case, increasing the slit size includes relatively more target flux from the wings than noise from the background, and the S/N keeps rising. The other gratings typically show a turn-over for slit heights between 5 and 10 pixels. The S/N loss by going from 5 to 10 pixel slit heights is typically only a few percent.

The simulations for a background level of 20% of the peak signal are in Figures 4a through e. The S/N loss above the critical slit height sets in at smaller slit height as compared with the 10% background case, since any added background noise is a larger fraction of the signal. The worst case is between 5000 and 6000 Å (both for grating G430L and G750L) where a slit height of 10 pixels leads to a S/N loss of nearly 10%. At longer wavelengths, increasing the slit height beyond 10 pixels results in less S/N loss, since the PSF is broader.

Finally, the case of a 50% background level is displayed in Figures 5a–e. The trends recognizable in the previous figures are present at an even stronger level. Significant (>10%) S/N degradation is found even for a slit height as short as 10 pixels.

4. Total flux versus slit height

The enclosed energy as a function of slit height is shown in Figures 6a-e for gratings G140L, G230L, G230LB, G430L, and G750L, respectively. From pre-launch studies, a value of 80% of the total flux was incorporated in the STIS Exposure Time Calculator (ETC, Hack et al. 1996) as a typical expectation for GO exposure planning purposes.

Figure 6a for G140L shows that for a slit height of 11 pixels, only about 70% of the total signal is extracted at most wavelengths, while for a height of 21 pixels, the total rises

to 80%. The figures assume a background distance of 300 pixel and a total flux of 100% at hgt=601 px. For G140L, a height of 21 would be required to achieve the expectations of the ETC. Because of low dark noise in a MAMA detector, little extra noise is added by the choice of a tall extraction slit. However, Figure 7 demonstrates that the extra ~10% of signal contains little spectral information, since the light in the wings at 12–21 px is scattered mainly from wavelengths removed from the bandpass of the instrumental resolution. To avoid this loss in resolution, a slit of 11 px is recommended. Even if the background is as high as 50% of the peak signal, a height of 11 will still retain $S/N > 95\%$ of the maximum at all wavelengths on the G140L grating.

Figure 6b for G230L shows that for a height of 11 pixels, a range of 73–81% is achieved. For a height of 21 pixels, the values rise by only ~10%. The PSF on the NUV-MAMA is narrower than in the FUV, because there is no repeller wire and less scattered light in the far wings of the PSF at longer wavelengths. Since the radiation induced background is much higher on the near-UV MAMA, brighter targets are effected by S/N considerations. At longer wavelengths for gratings G230LB (Figure 6c) and G430L (Figure 6d), more than 80% of the enclosed energy is contained in 7 pixels for gratings G230LB and G430L.

Figure 6e for G750L illustrates the most problematic CCD case, where the PSF blooms in the IR. At one micron, a slit height of 7 pixels captures only 53% of the signal, while a height of 21 improves to only 65%. A slit height of about 60 pixels is required to get 80% of the fractional energy.

5. Recommendations

There is no slit height that would optimize the encircled energy and the S/N for any target brightness. Based on the curves in Figures 2, 5, and 6, Table 2 illustrates the trade-offs. The first two columns of this table list the grating modes and wavelengths. Column 3 gives the enclosed energy (in %) for slit heights of 11 (G140L, G230L) and 7 pixels (G230LB, G430L, G750L). Columns 4, 5, and 6 are from Figure 3, which refers to the 10% background case. Column 4 gives the S/N relative to the peak- S/N (in percent) reached at 11 pixels (G140L, G230L) and 7 pixels (G230LB, G430L, G750L). The S/N relative to the peak- S/N (in percent) for a slit height of 4 pixels is in column 5, and the corresponding quantity at a height of 20 pixels is in column 6. Slit heights of 4 and 20 pixels bracket the pixel number where the maximum S/N occurs in essentially all cases. However, a slit height of less than 7 pixels causes degraded photometric precision due to non-repeatability among observations of the same standard star. The case of a 50% background (from Figure 5) is treated in columns 7, 8, 9. The entries in these columns are defined analogous to those in columns 4, 5, and 6.

The enclosed target energy is independent of the background level, whereas the S/N vs. slit height relation is a strong function of the target brightness relative to the back-

ground rate. Since our goal is to define a slit height that would fit most needs, and at the same time has as few variables as possible, our slit selection is guided by the requirement to maximize photometric precision and spectral purity. How this choice affects the S/N is discussed below.

A slit height of 11 pixels for the G140L and G230L gratings and 7 pixels for the other gratings retains ~80% of the enclosed energy (the ETC value) for most wavelengths, except for G140L and the longer wavelengths of G750L. Extraction of larger fractions of the signal would require slits that would degrade spectral purity or reduce the S/N for background dominated cases.

If background is negligible, the conditions for maximizing the encircled energy and the S/N are identical: a slit height as large as possible is desired; but recall that the slit for which 80% of the energy is reached, will result in a fractional S/N of 89% of the maximum.

Cases with background are more interesting. For the case of a 10% background, Table 2 (column 4) suggests that slit heights of 11 (MAMA modes) and 7 (CCD modes) pixels are close to the slit heights that maximize S/N; alternatively, the S/N vs. slit relation has such a small gradient that a S/N loss of less than 5% occurs due to the chosen, non-optimal slit height. Slit heights less than 7 pixels are not desirable due to non-repeatability of the photometry.

The case of a 50% background is comparable to the 10% case for the suggested slit heights. The slit height for which the S/N is maximum, generally is at slightly smaller heights (column 7). If the background were even higher, the achieved S/N relative to the maximum possible would be even lower for the selected slit heights.

For most applications, slit heights of 11 pixels for G140L and G230L, and 7 pixels for G230LB, G430L, and G750L give satisfactory results. If the target has count rates that are comparable to the background, smaller slit heights should be selected to improve the S/N and visibility of spectral features. Table 2 provides guidance for selecting the optimum slit height.

6. References

- Hack, W., Sahu, K. Kinney, E., & Bohlin, R. 1996, Instrument Science Report, STIS 96-020, (Baltimore:STScI).
- Horne, K., 1986, *PASP*, 98, 609.
- Kinney, A. L., Bohlin, R. C., & Neill, J. D. 1991, *PASP*, 103, 694.

Table 2. Comparison of enclosed energy and S/N for different gratings and wavelengths.

1	2	3	4	5	6	7	8	9
			BKG=0.1			BKG=0.5		
Grating	Wavelength (Å)	Energy (11,7) (%)	S/N (11,7) (%)	S/N (4) (%)	S/N (20) (%)	S/N (11,7) (%)	S/N (4) (%)	S/N (20) (%)
G140L	1183	65	94	75	99	100	87	98
	1299	72	98	83	100	99	92	92
	1416	73	100	90	99	97	95	87
	1533	73	100	89	99	98	97	86
	1649	73	100	89	99	98	96	87
	1693	73	100	89	99	98	96	87
G230L	1732	73	99	83	99	98	91	90
	2041	77	100	89	98	96	95	86
	2350	79	100	90	97	95	97	83
	2660	80	100	90	96	95	97	82
	2969	82	100	90	96	95	97	82
	3085	82	100	90	96	95	97	82
G230LB	1808	80	99	91	96	100	96	82
	2082	82	100	95	93	96	99	75
	2357	83	100	95	95	96	99	76
	2631	83	100	95	92	96	97	<75
	2906	84	100	95	92	96	99	<75
	3009	84	100	95	92	96	99	<75
G430L	3175	87	100	96	90	95	99	<75
	3724	88	100	96	90	95	99	<75
	4272	88	99	96	90	95	99	<75
	4821	88	99	96	90	95	98	<75
	5370	88	99	96	90	95	99	<75
	5575	88	99	96	90	95	99	<75
G750L	5752	90	99	97	88	95	99	<75
	6728	88	100	95	91	98	98	<75
	7703	84	100	93	92	100	98	76
	8678	74	100	91	94	100	97	80
	9654	63	98	89	96	100	95	83
	10020	53	98	88	98	100	95	86

7. Figure Captions

Figure 1. Cross-sections of the signal distribution perpendicular to the dispersion direction. Each PSF is normalized to a peak value of 100. a) Grating G140L at six wavelengths from 1183 Å to 1693 Å. b) Grating G230L at six wavelengths from 1732 Å to 3085 Å. c) Grating G230LB at six wavelengths from 1808 Å to 3009 Å. d) Grating G430L at six wavelengths from 3175 Å to 5575 Å. e) Grating G750L at six wavelengths from 5752 Å to 10020 Å; the strong wavelength dependence of the PSF provides a clean separation of the six curves for the G705L grating. For the definition of the line types, see Figure 2.

Figure 2. S/N as a function of extraction slit height for six different wavelengths. Each curve is normalized to its peak value. The background is zero. a) G140L. b) G230L. c) G230LB. d) G430L. e) G750L.

Figure 3. Same as Figure 2 but for a background of 10% the peak signal.

Figure 4. Same as Figure 2 but for a background of 20% the peak signal.

Figure 5. Same as Figure 2 but for a background of 50% the peak signal.

Figure 6. Enclosed energy as a function of slit height for six different wavelengths. Each curve is normalized to be 100% of the total signal at height=600. a) G140L. b) G230L. c) G230LB. d) G430L. e) G750L.

Figure 7. The region around the CII line at 1335 Å in GRW+70°5824 with extraction slit heights of 11 and 21 pixels (light lines). The heavy line is the differential signal at the ends of the extraction slit from 12-21 px. This extra signal is multiplied by seven for comparison purposes and shows a poor spectral purity, i.e., the CII line profile does not track the spectrum in the core of the PSF. The curves are smoothed twice with a box width of three pixels.

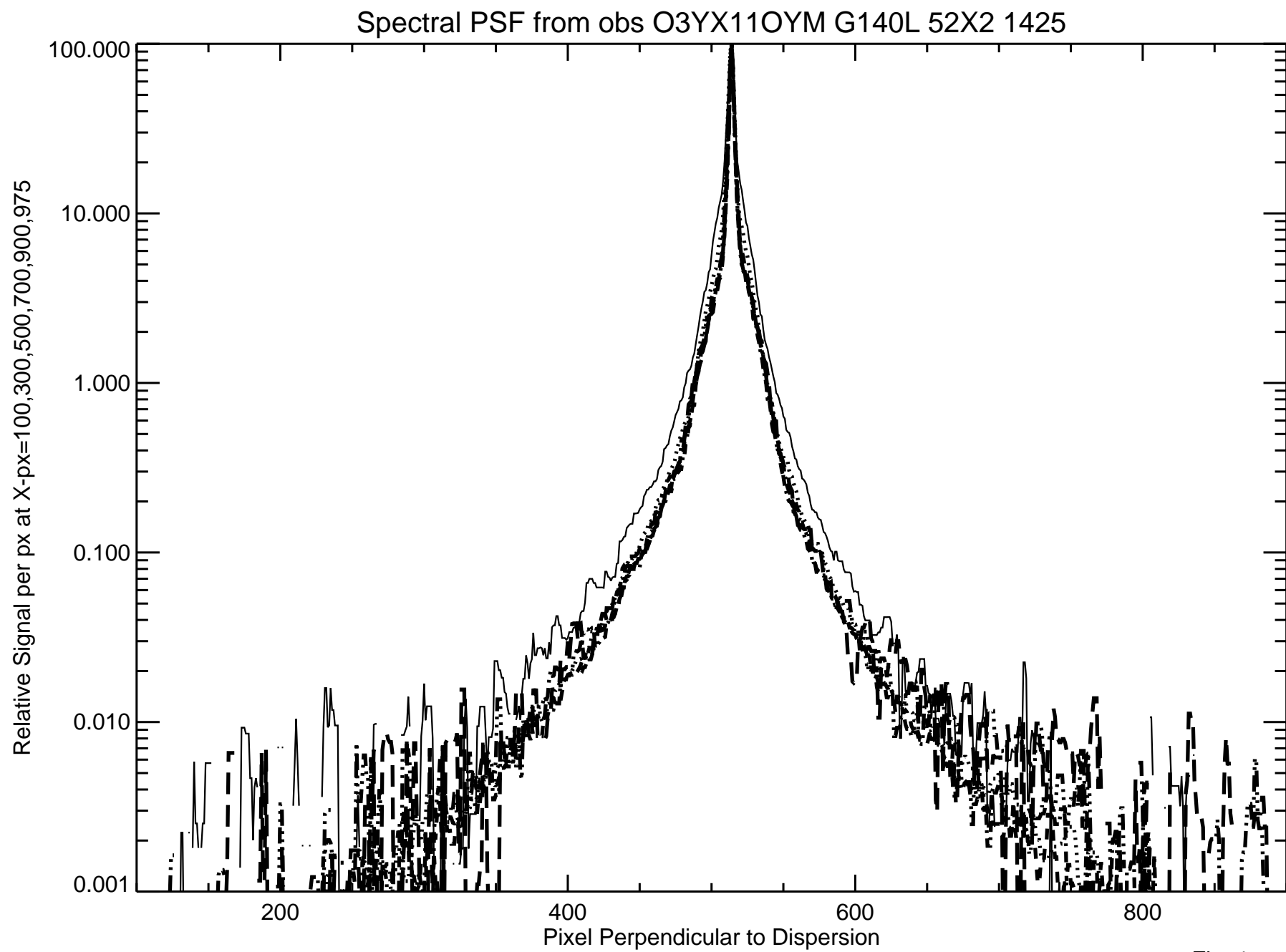


Fig. 1a

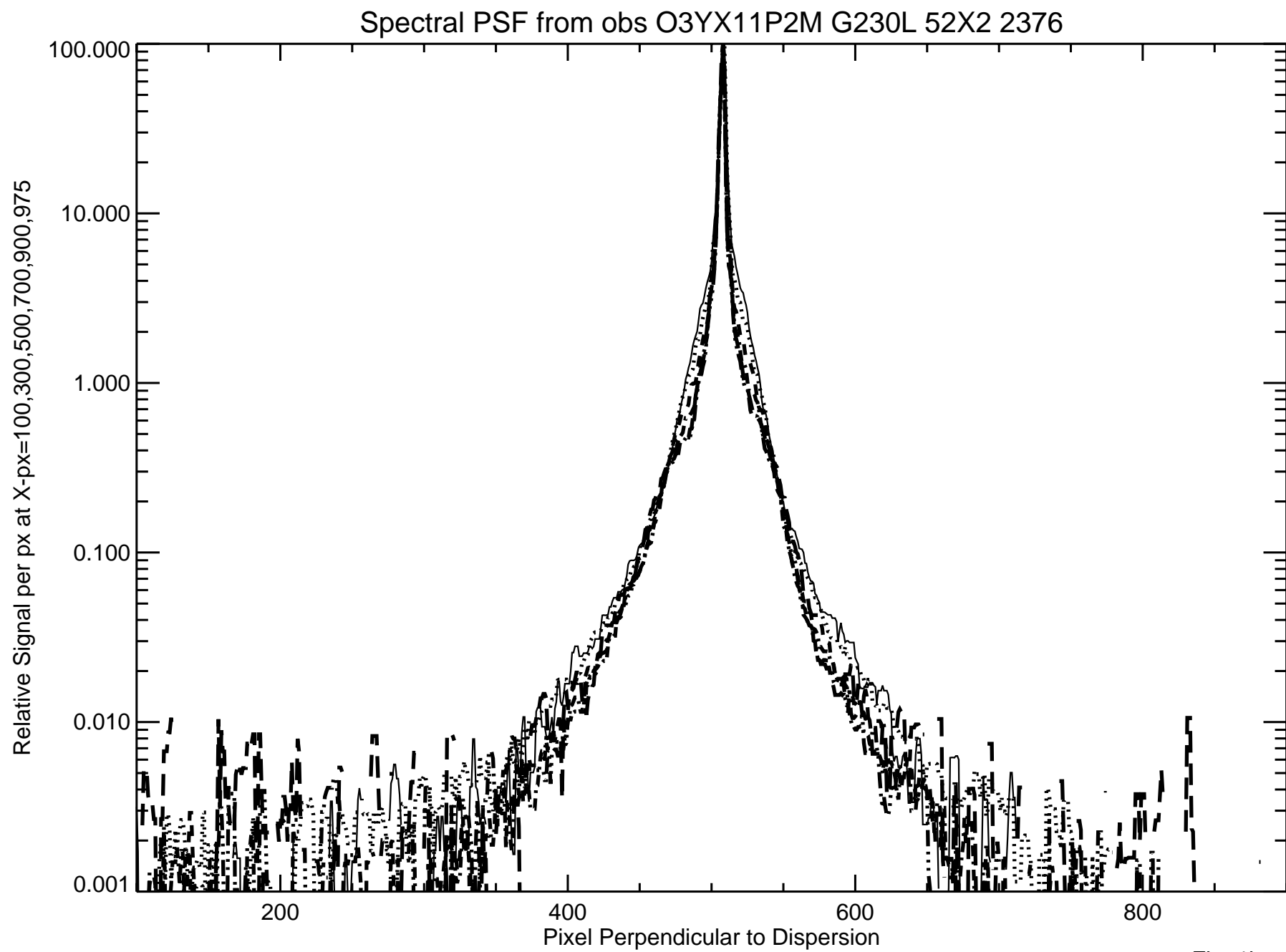


Fig. 1b

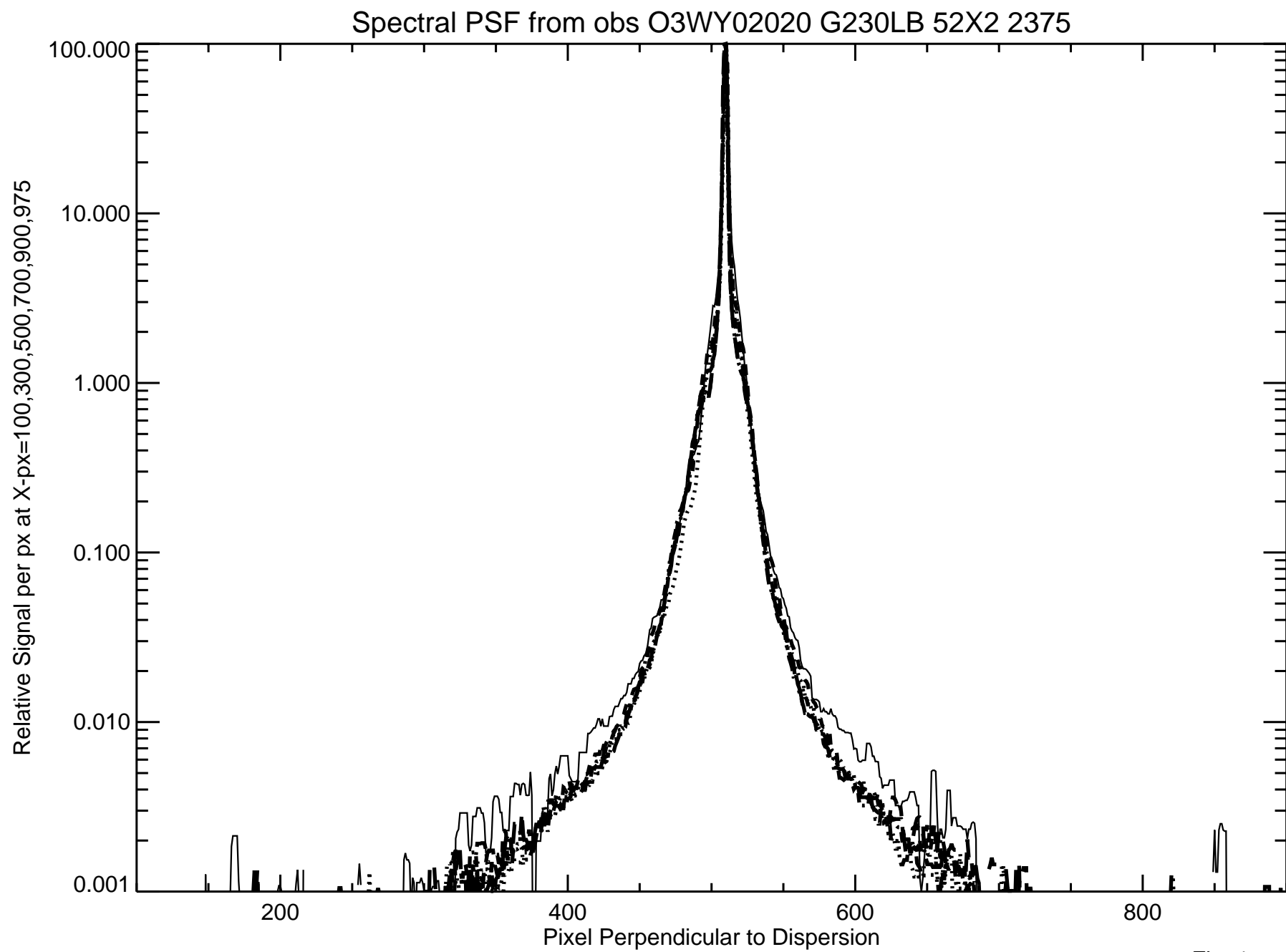


Fig. 1c

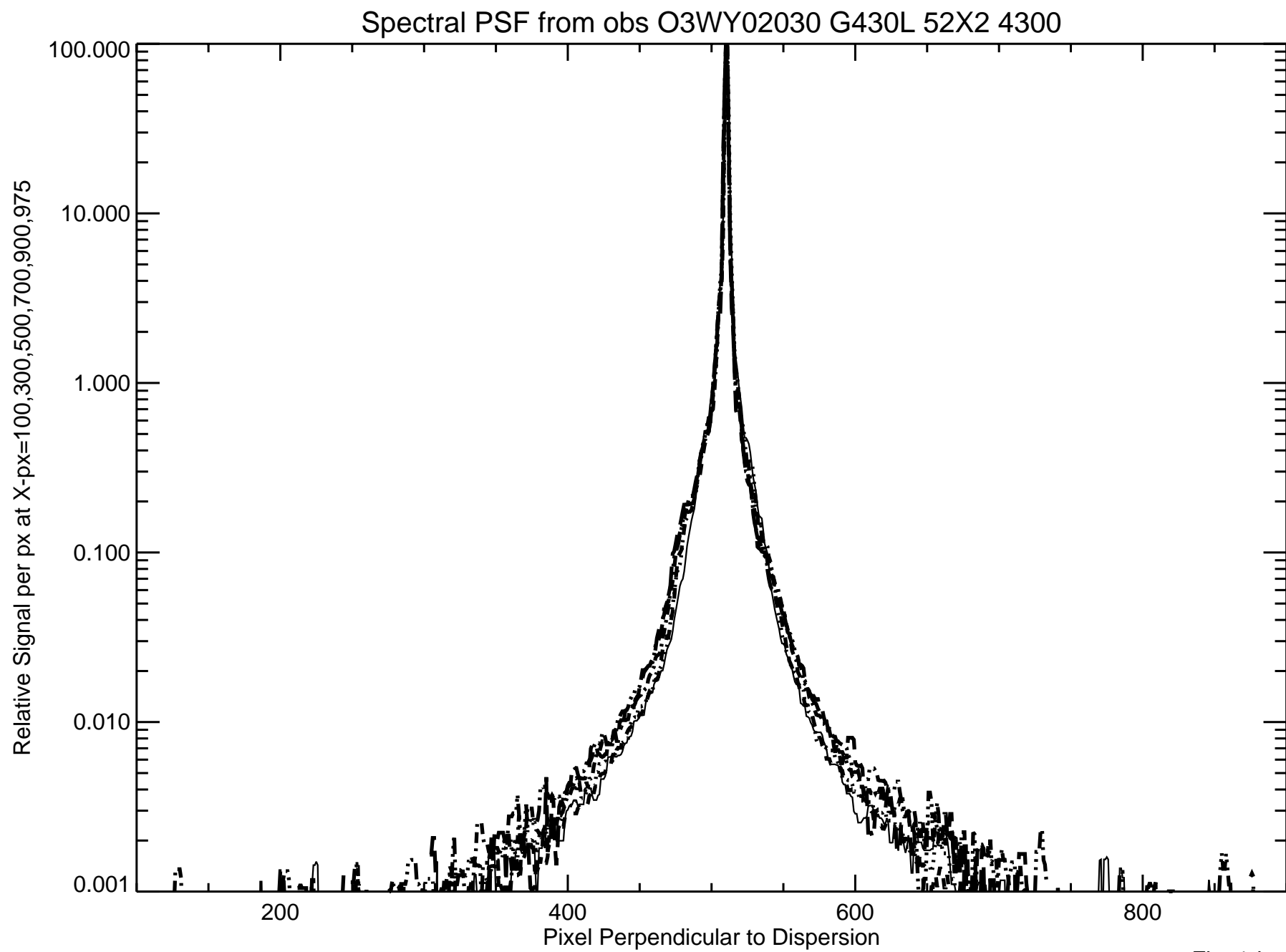


Fig. 1d

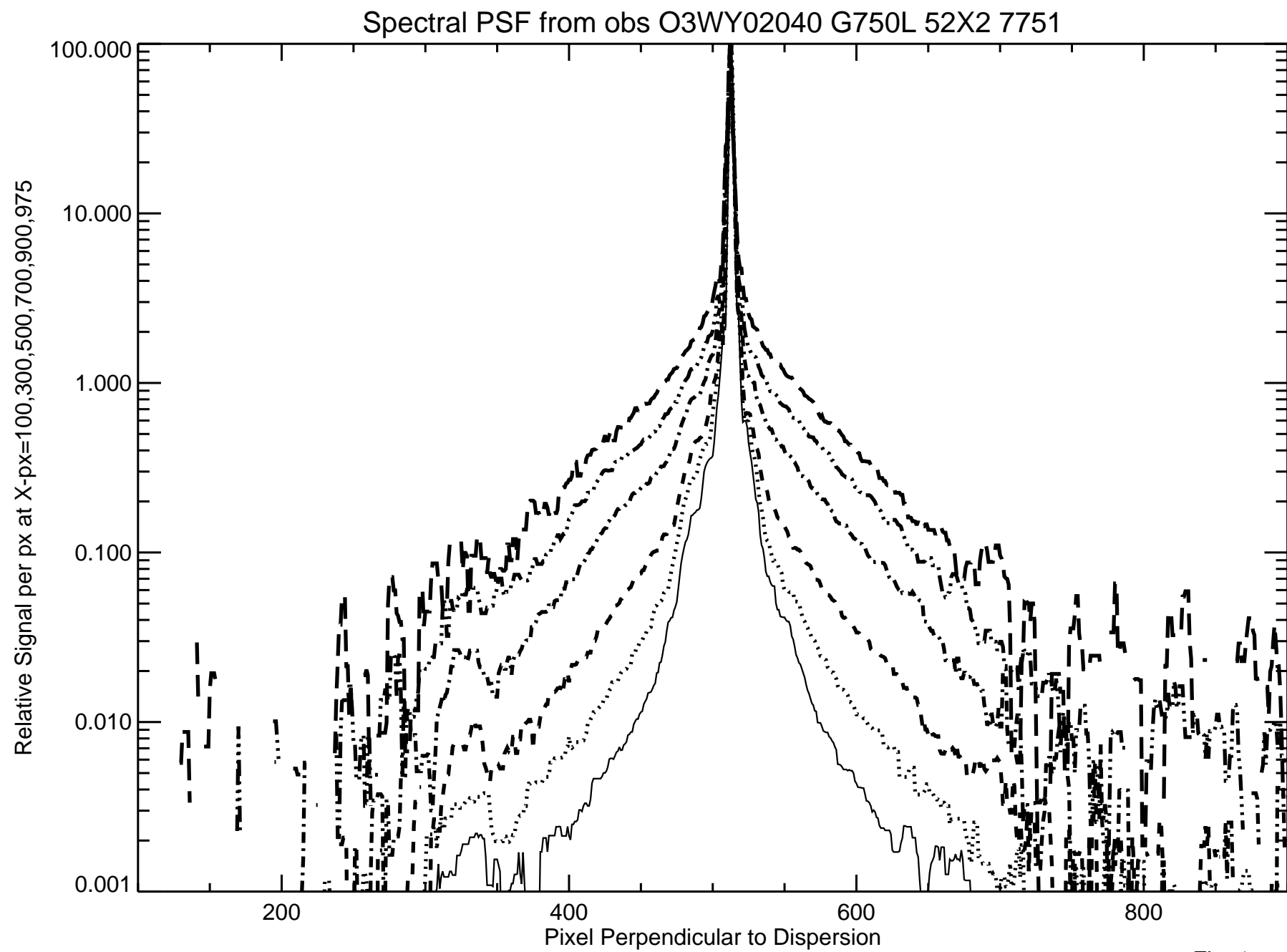


Fig. 1e

Spectral PSF from obs O3YX11OYM G140L 52X2 1425

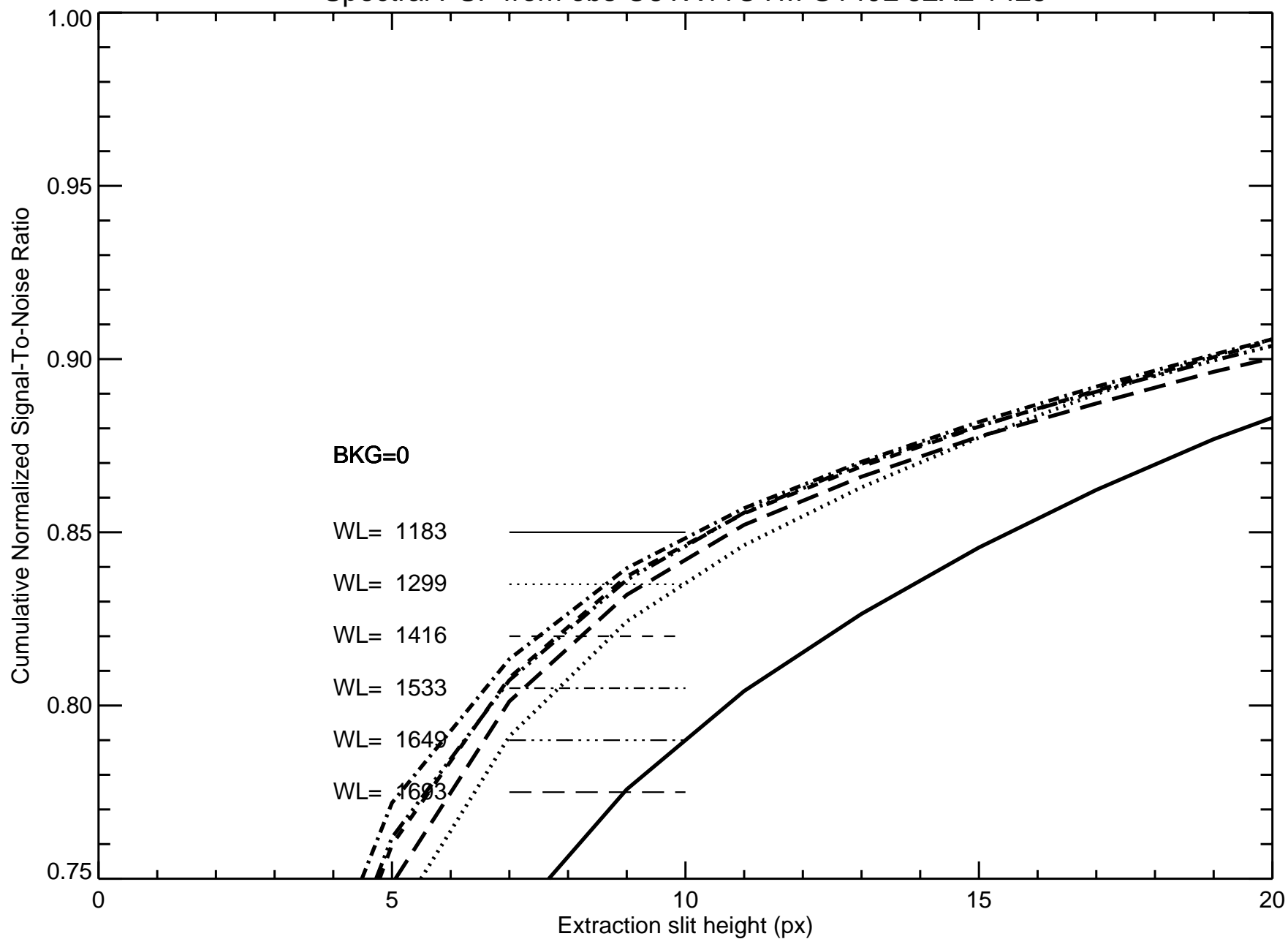


Fig. 2a

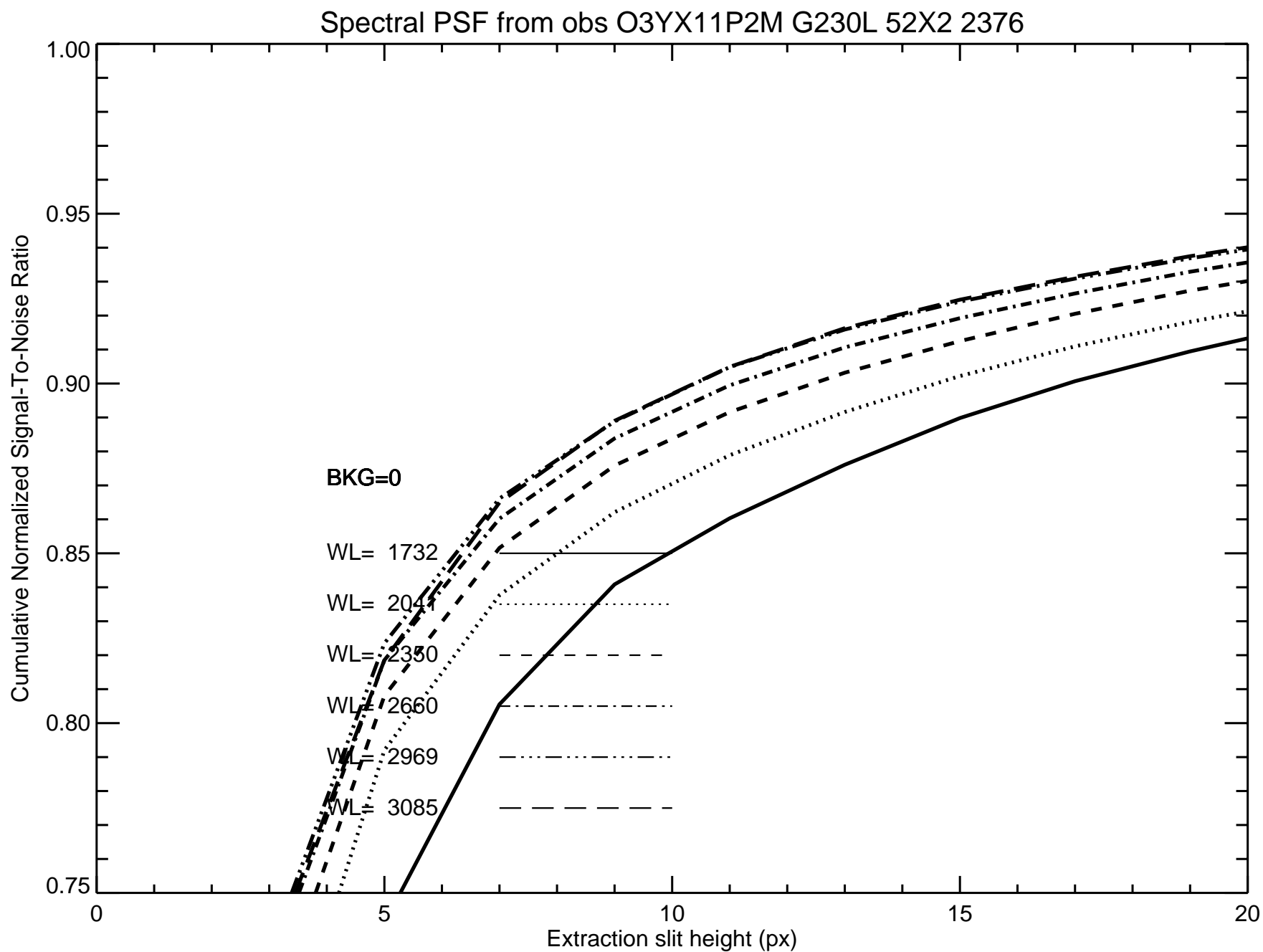


Fig. 2b

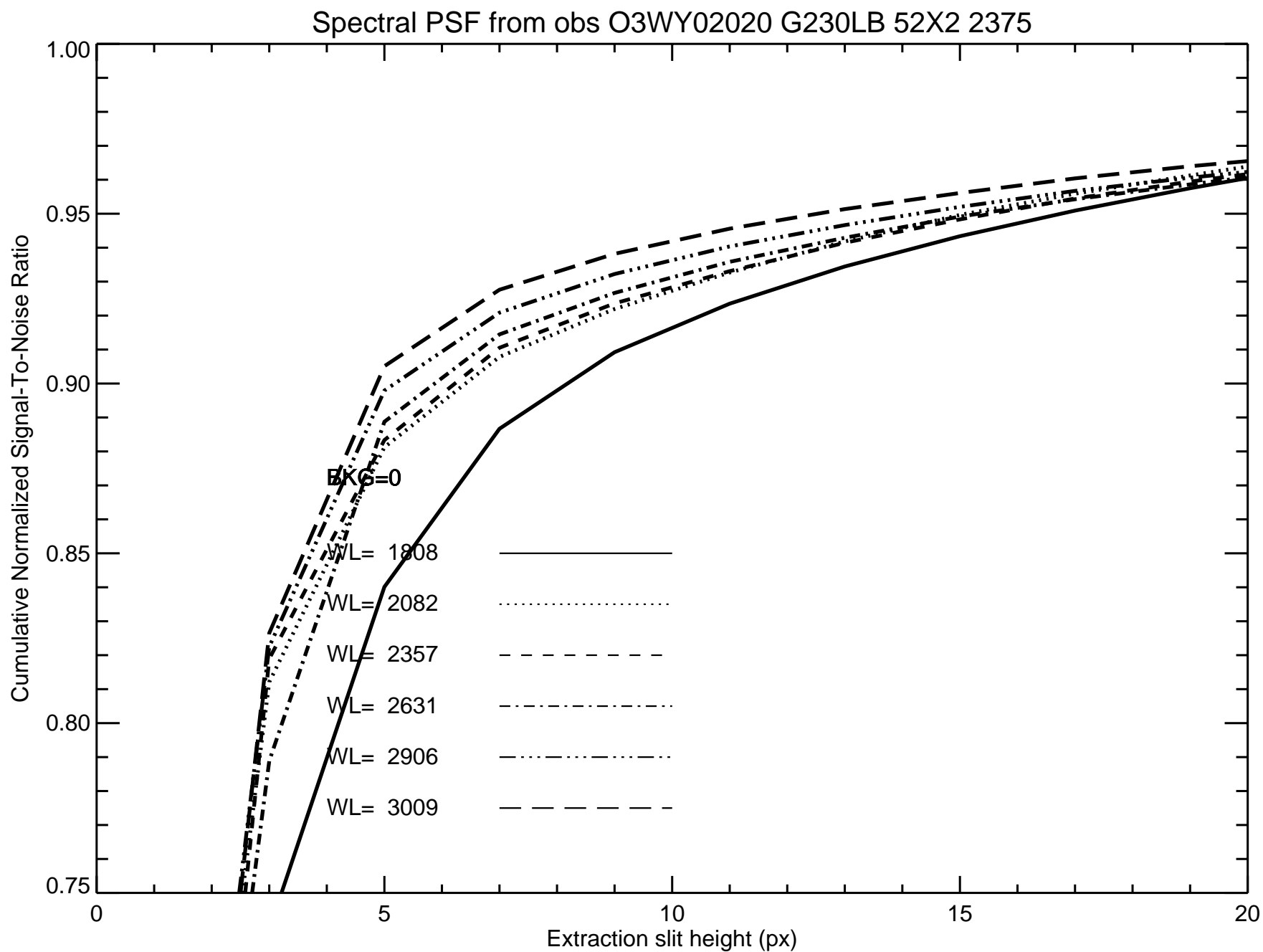


Fig. 2c

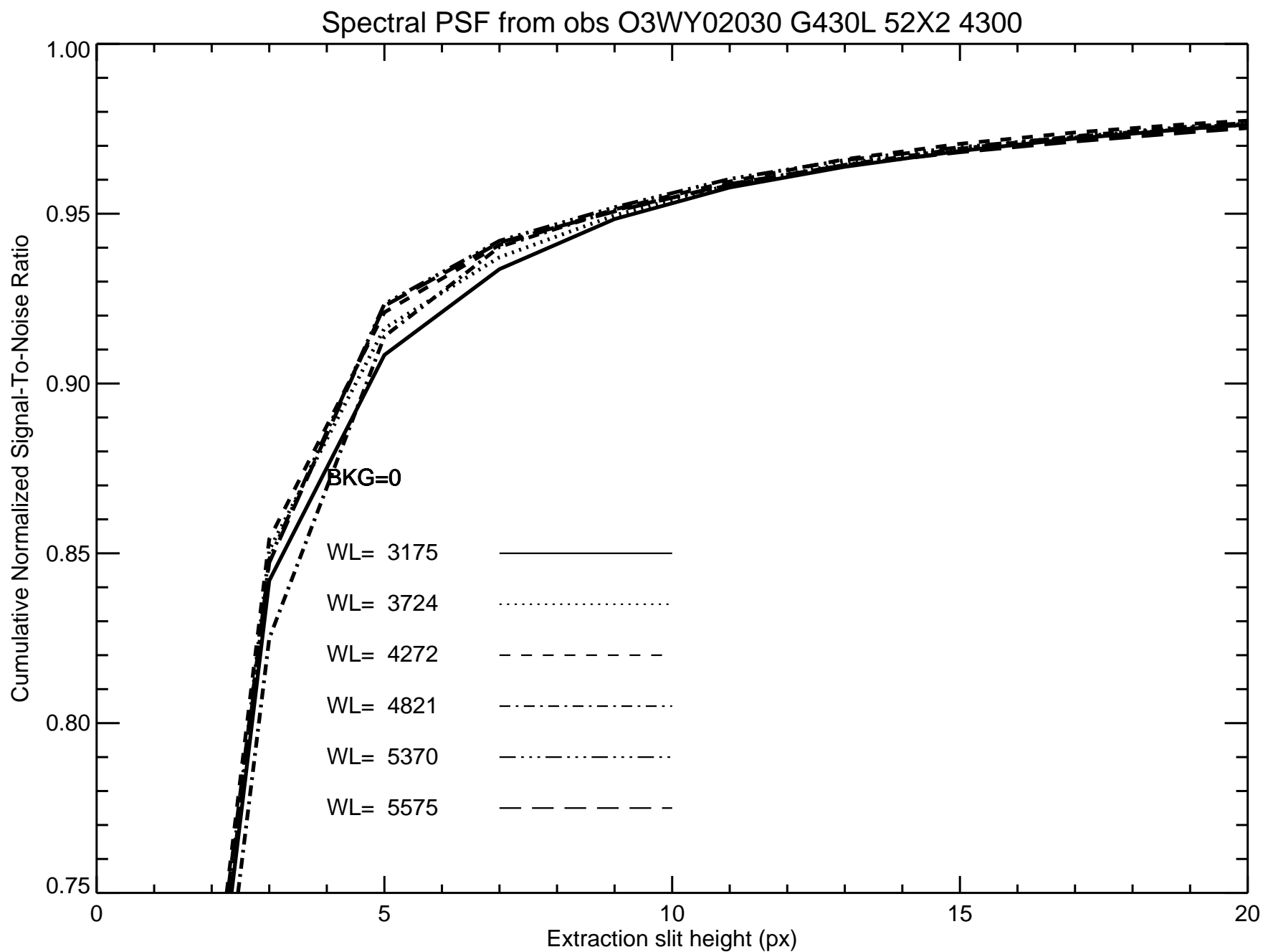


Fig. 2d

Spectral PSF from obs O3WY02040 G750L 52X2 7751

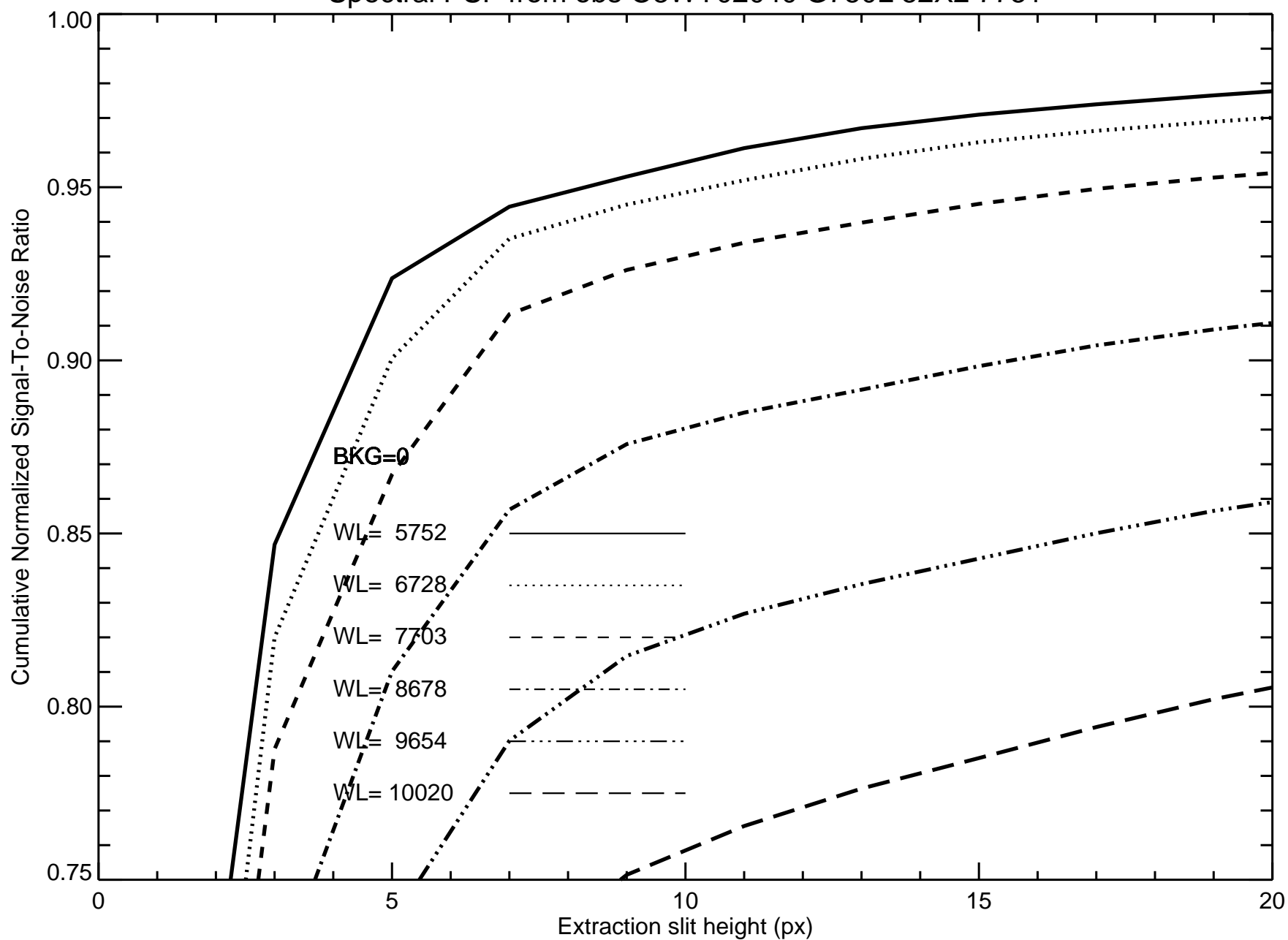


Fig. 2e

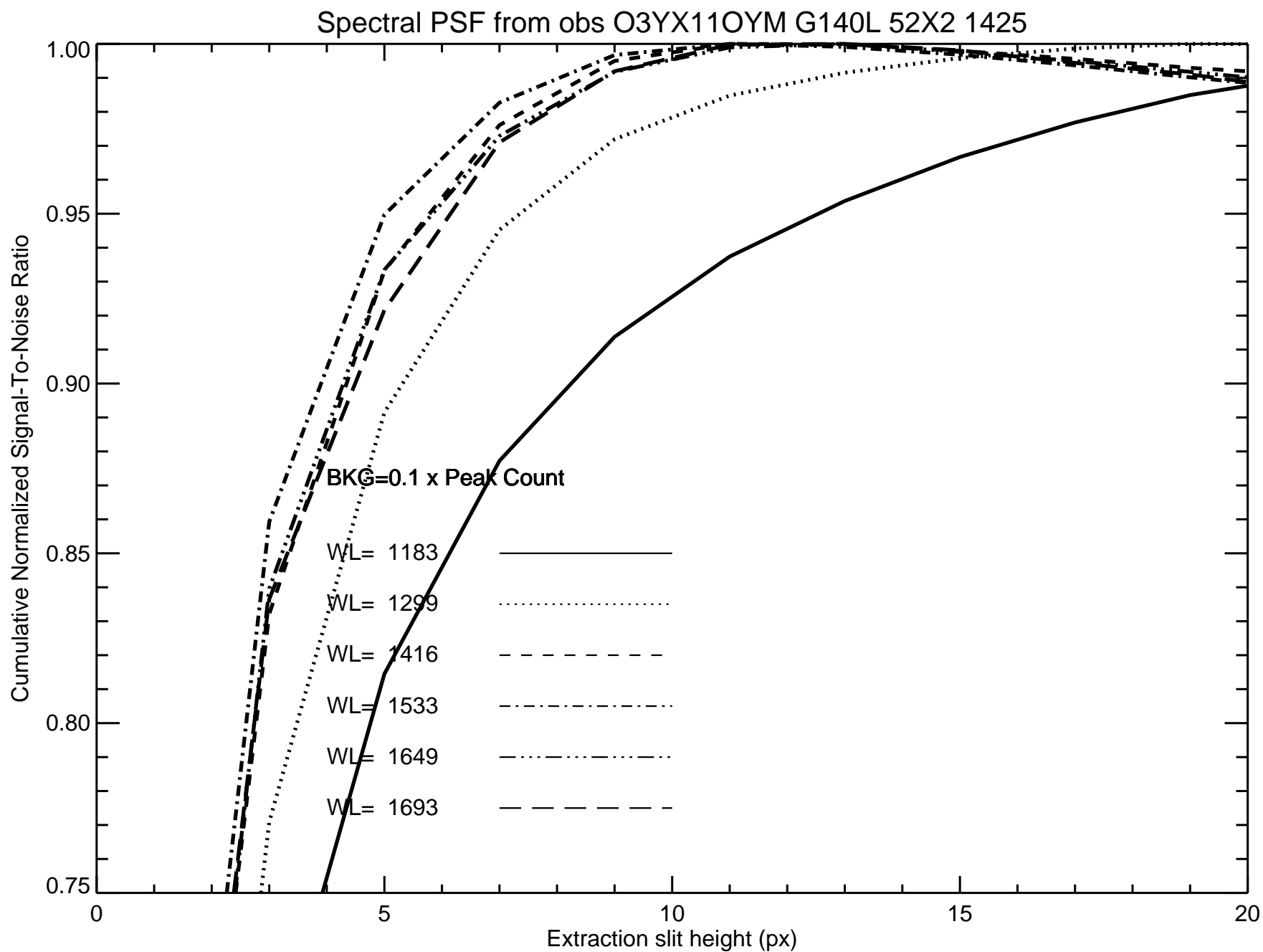


Fig. 3a

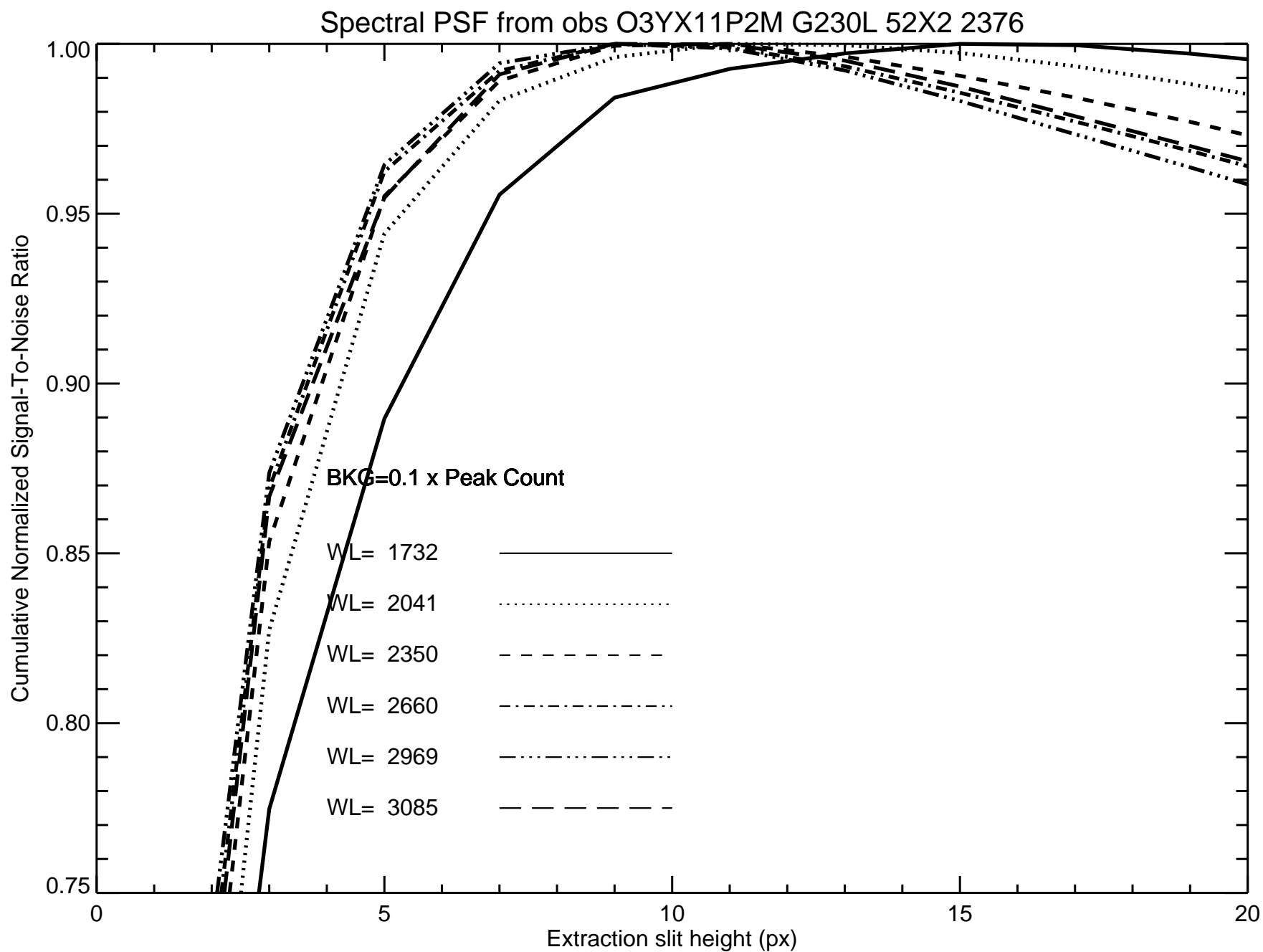


Fig. 3b

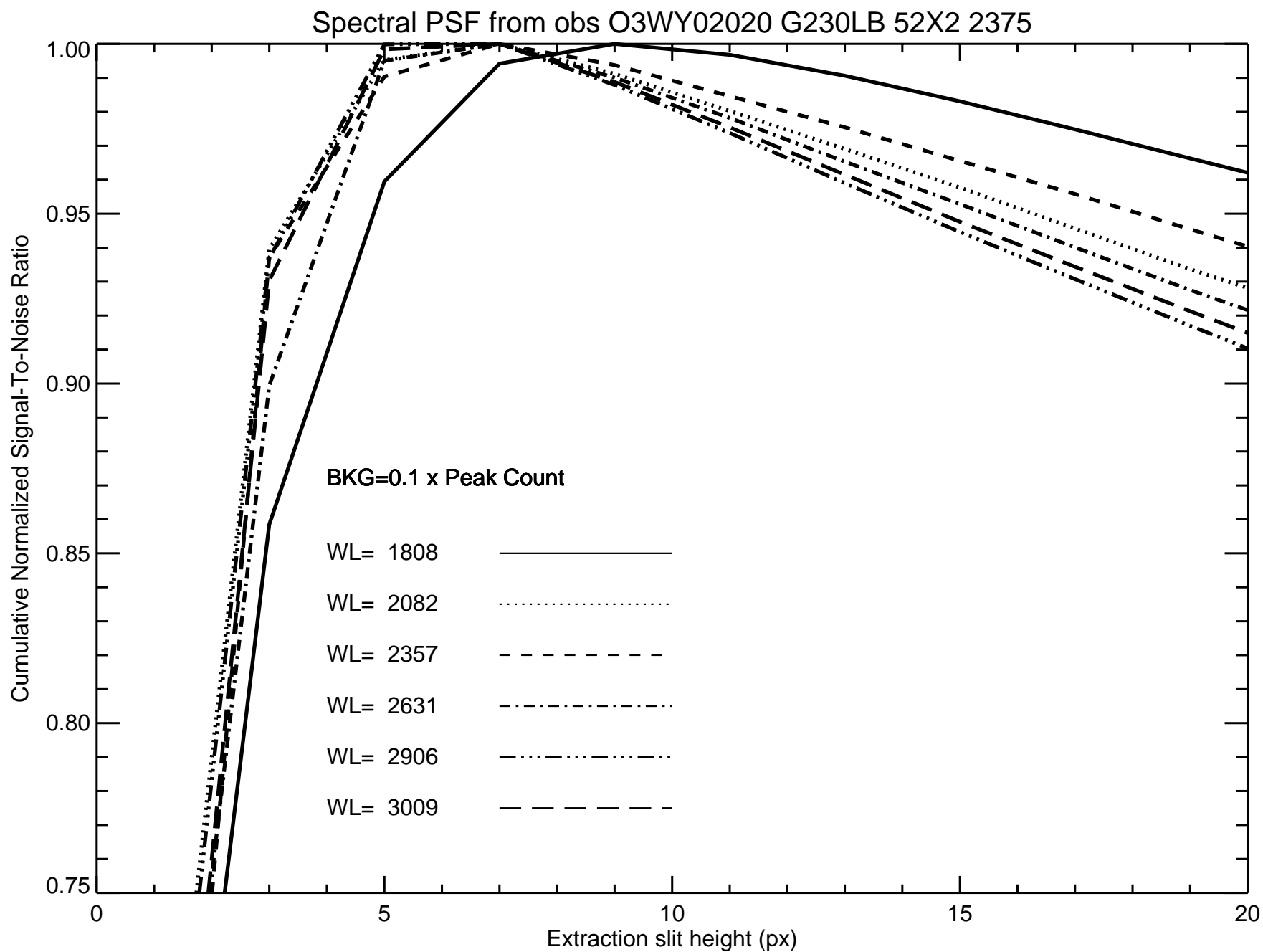


Fig. 3c

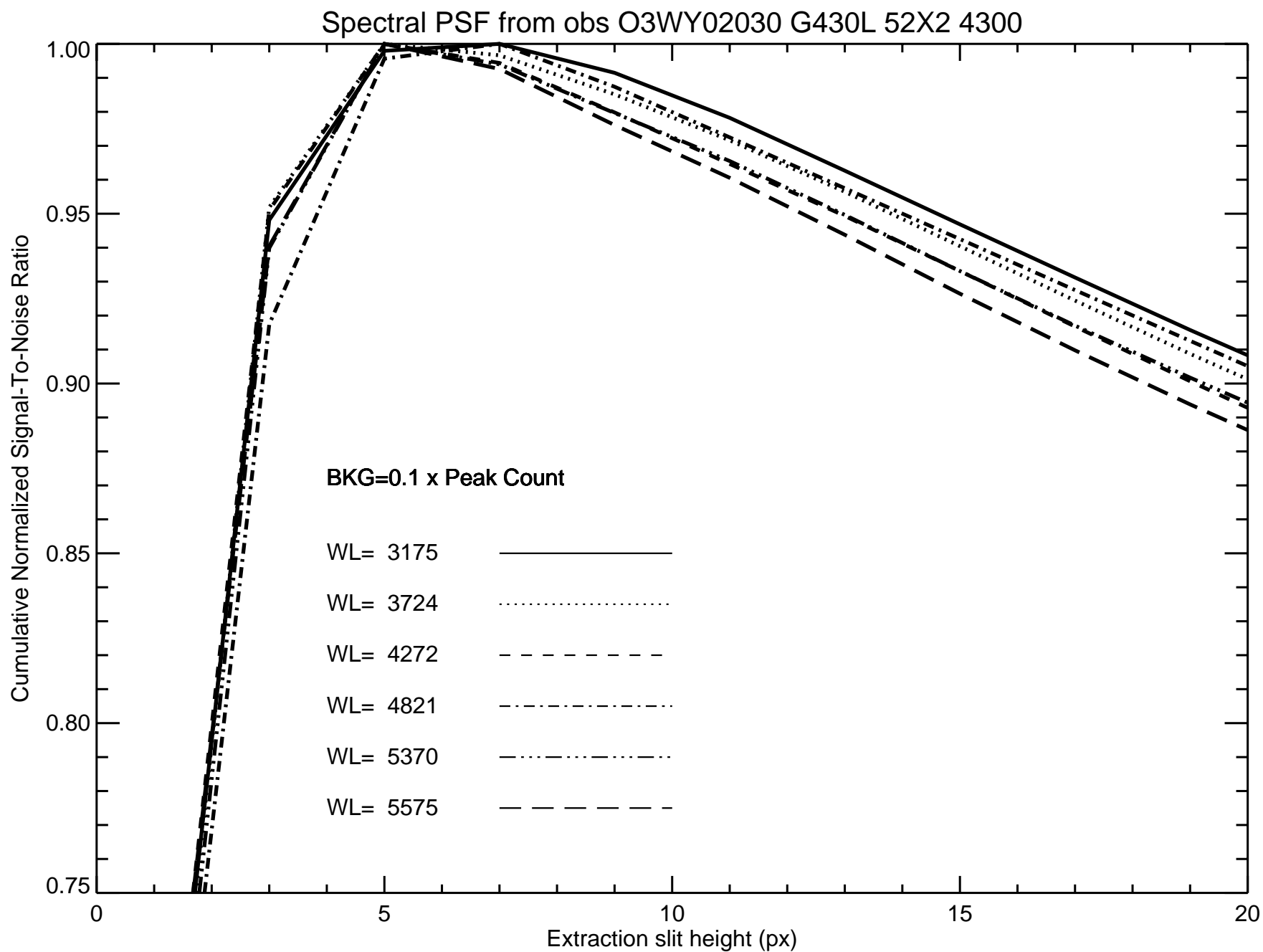


Fig. 3d

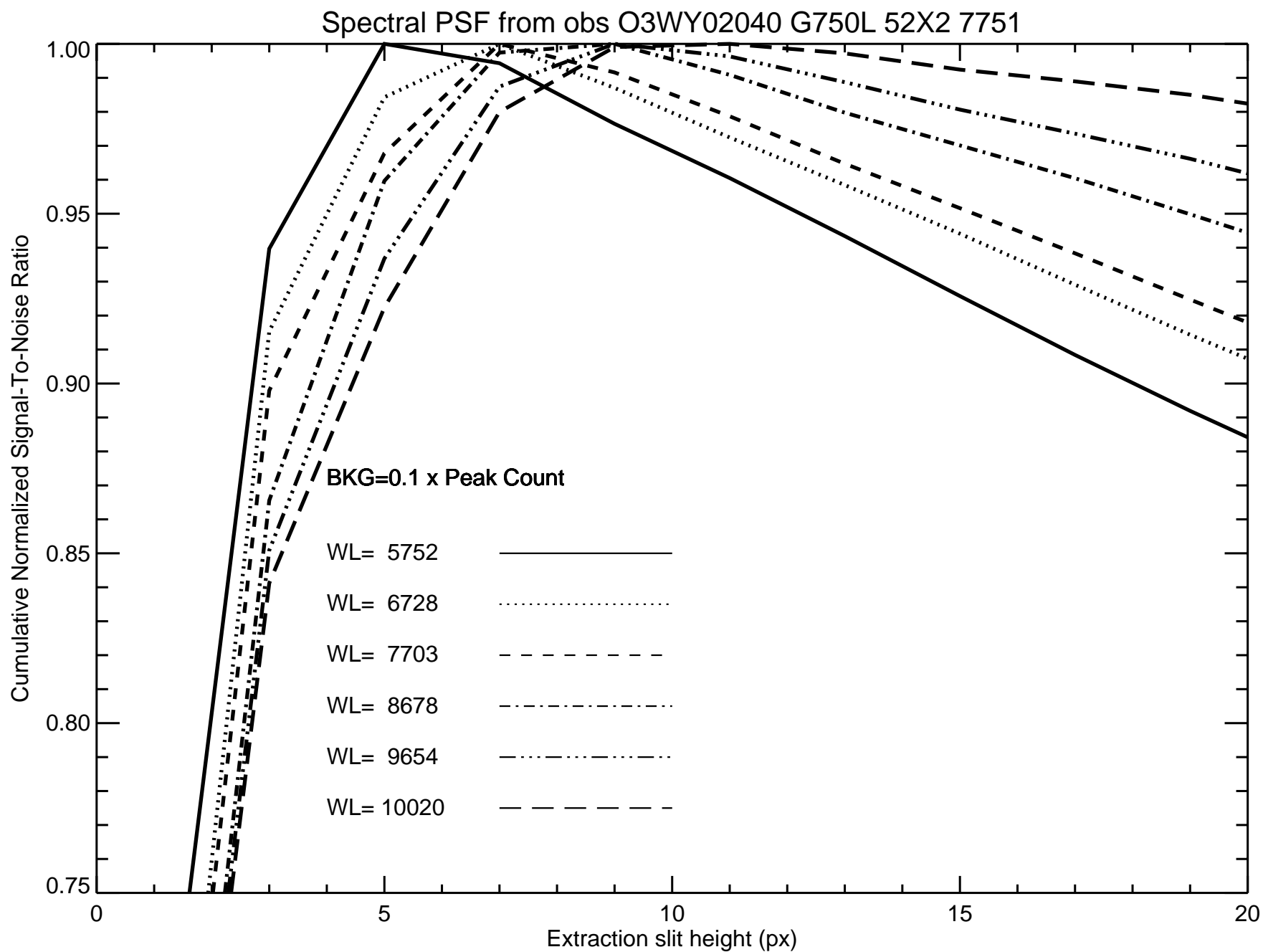


Fig. 3e

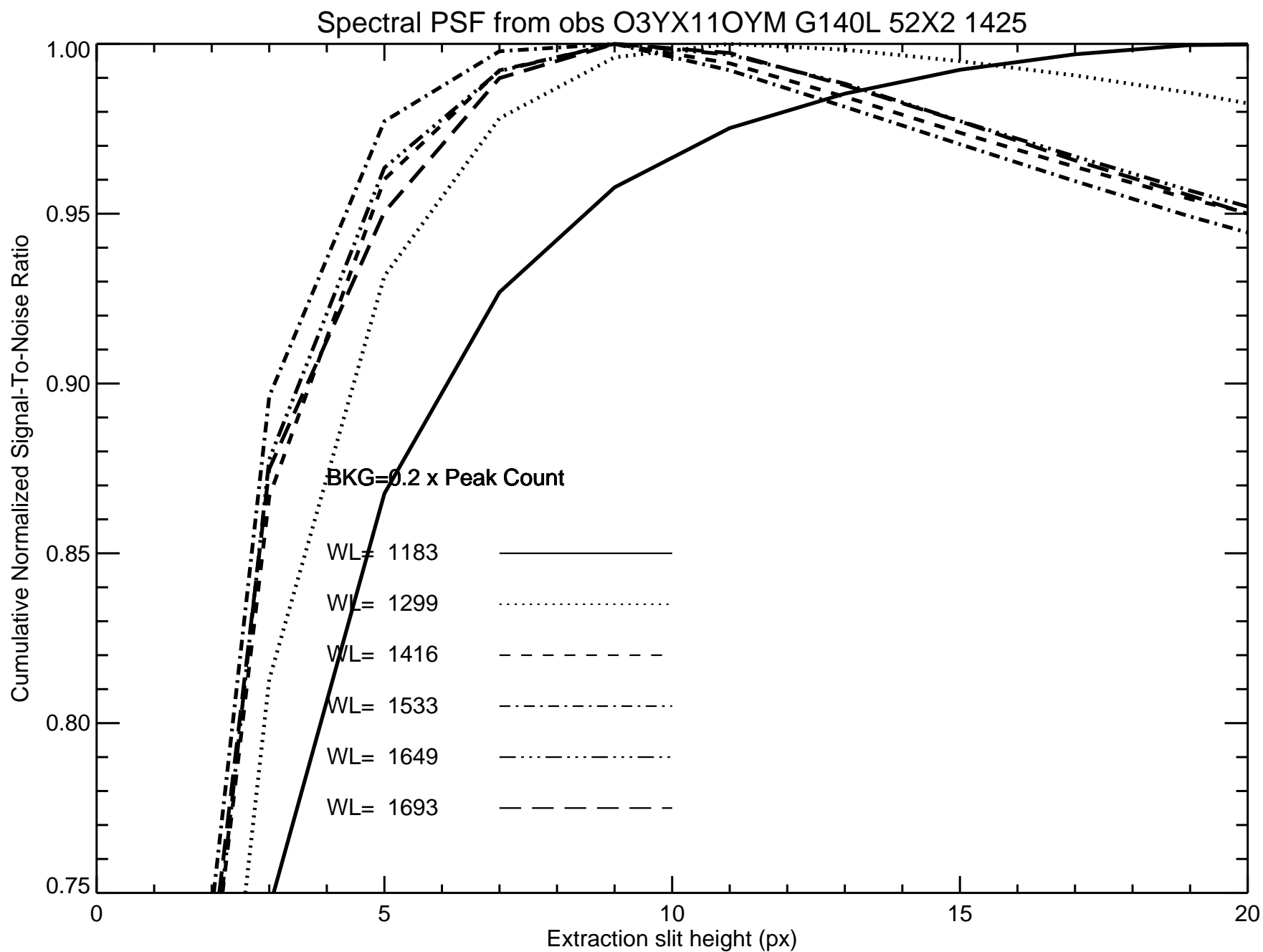


Fig. 4a

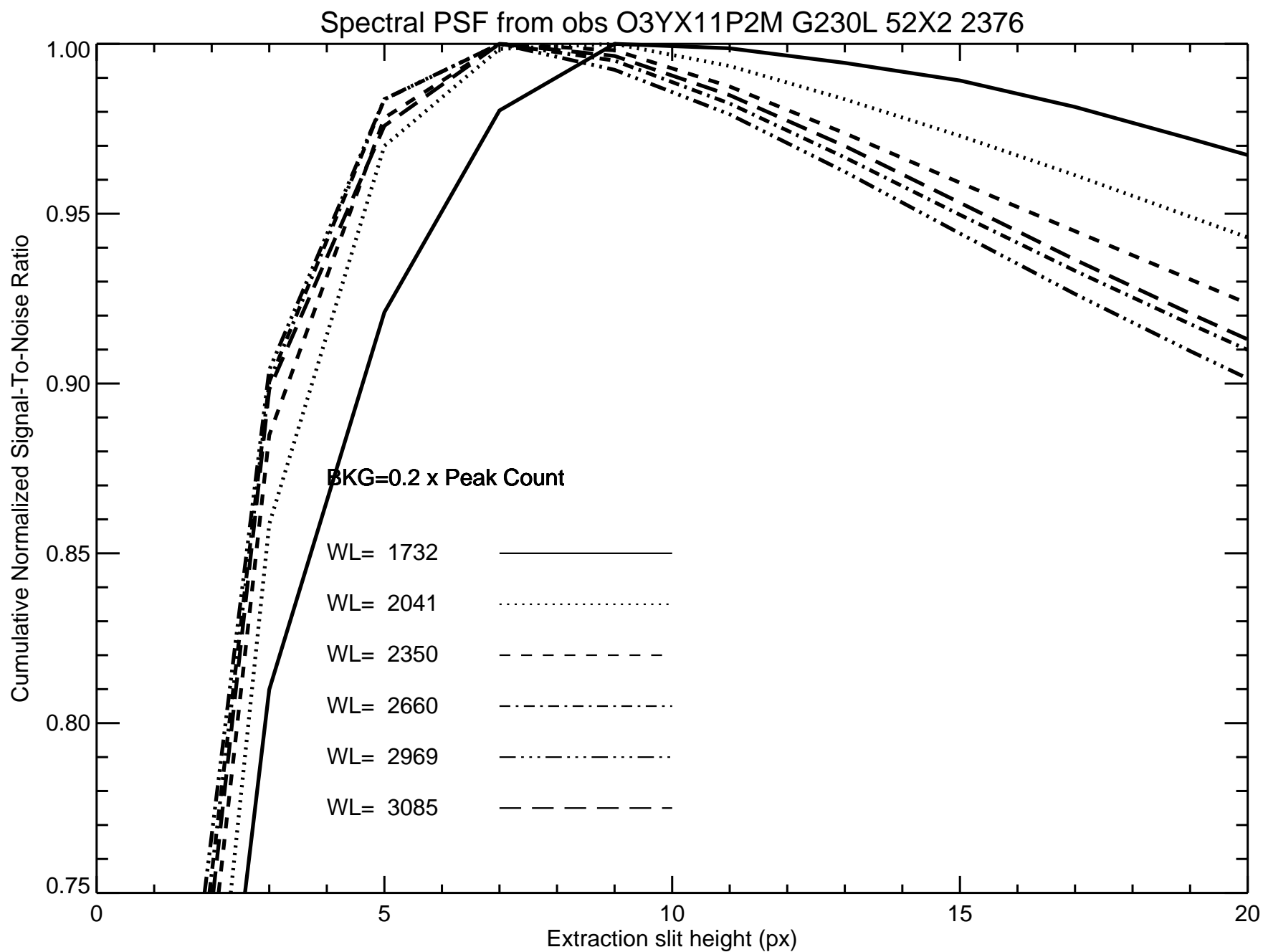


Fig. 4b

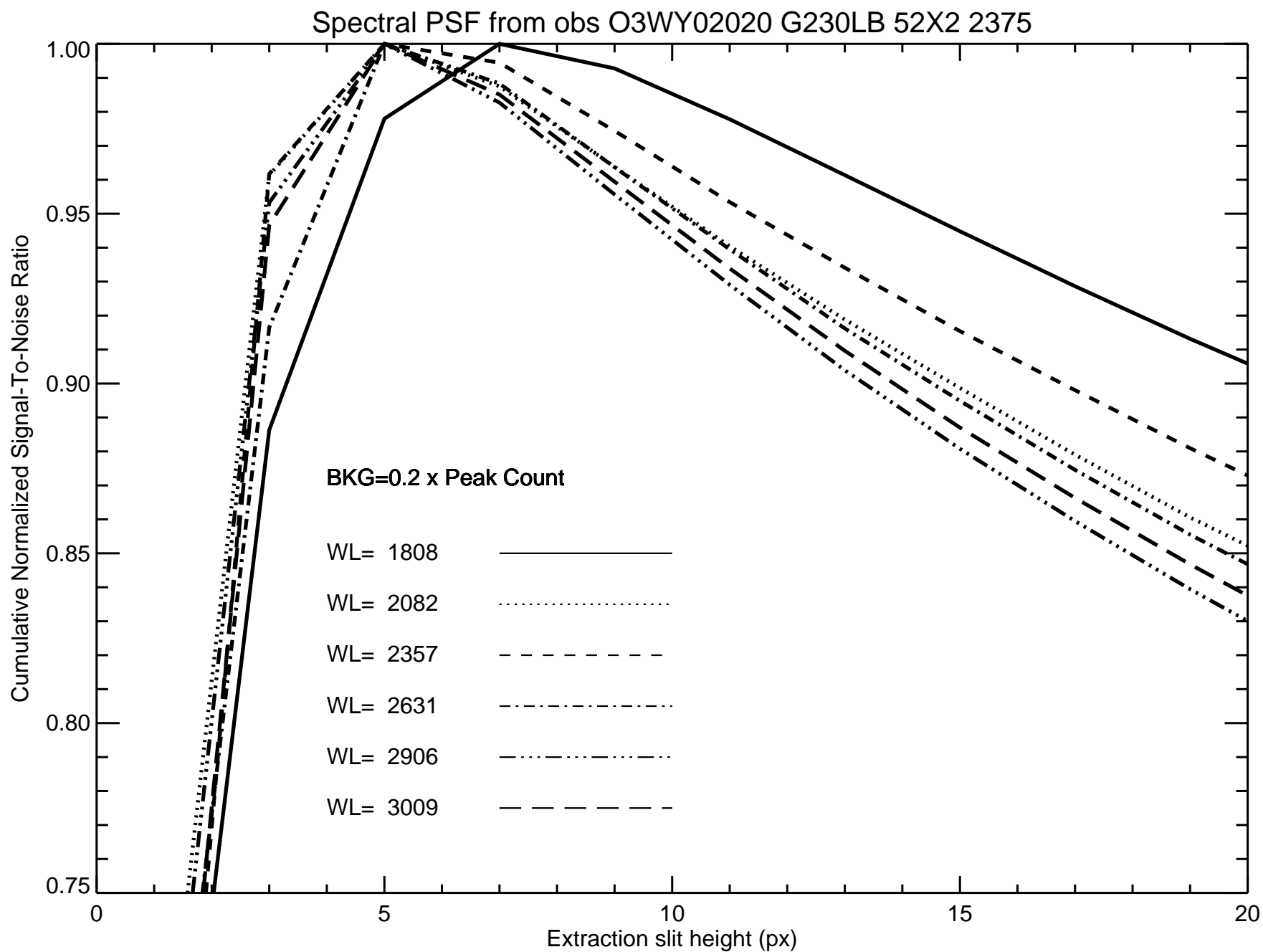


Fig. 4c

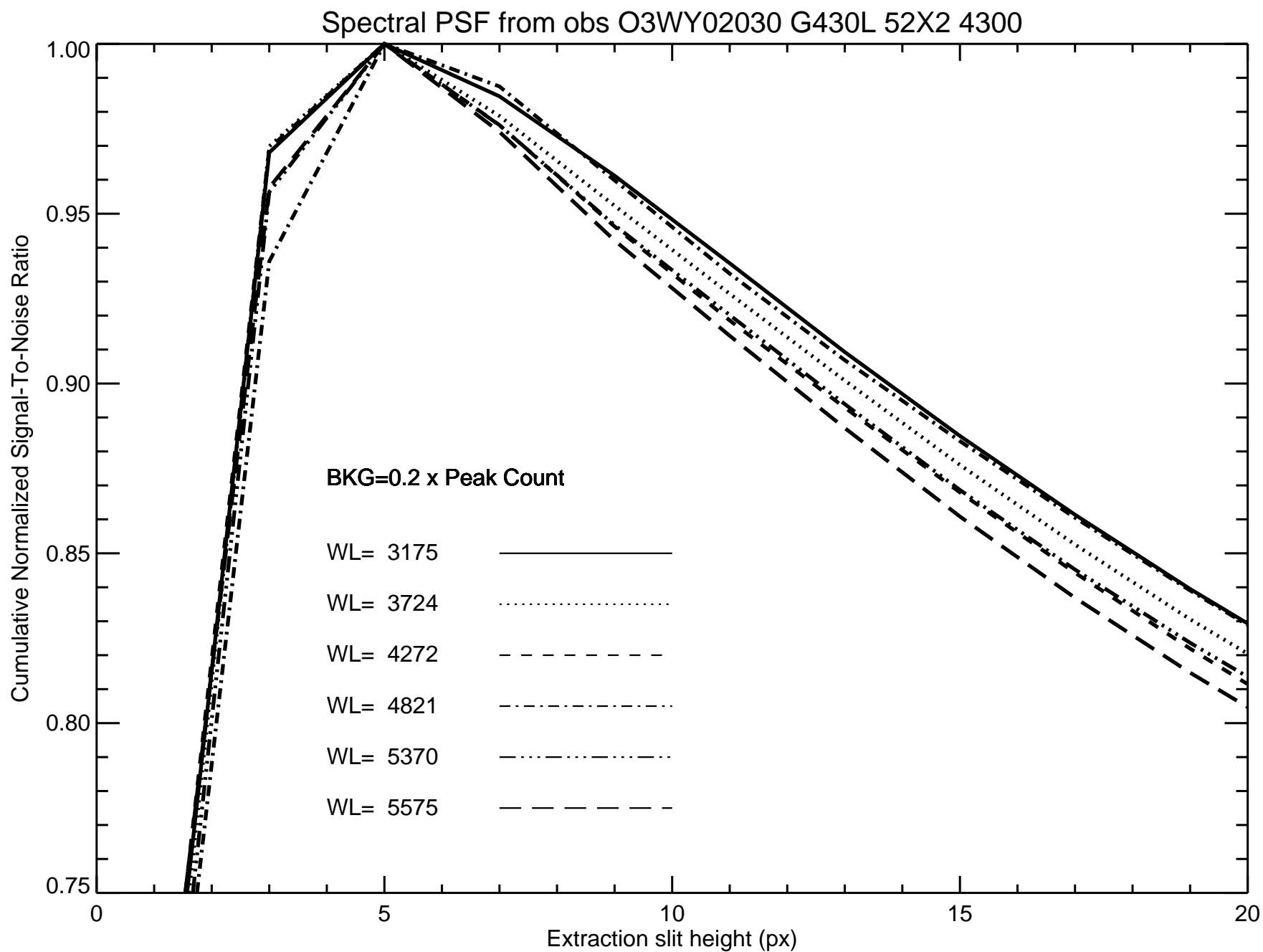


Fig. 4d

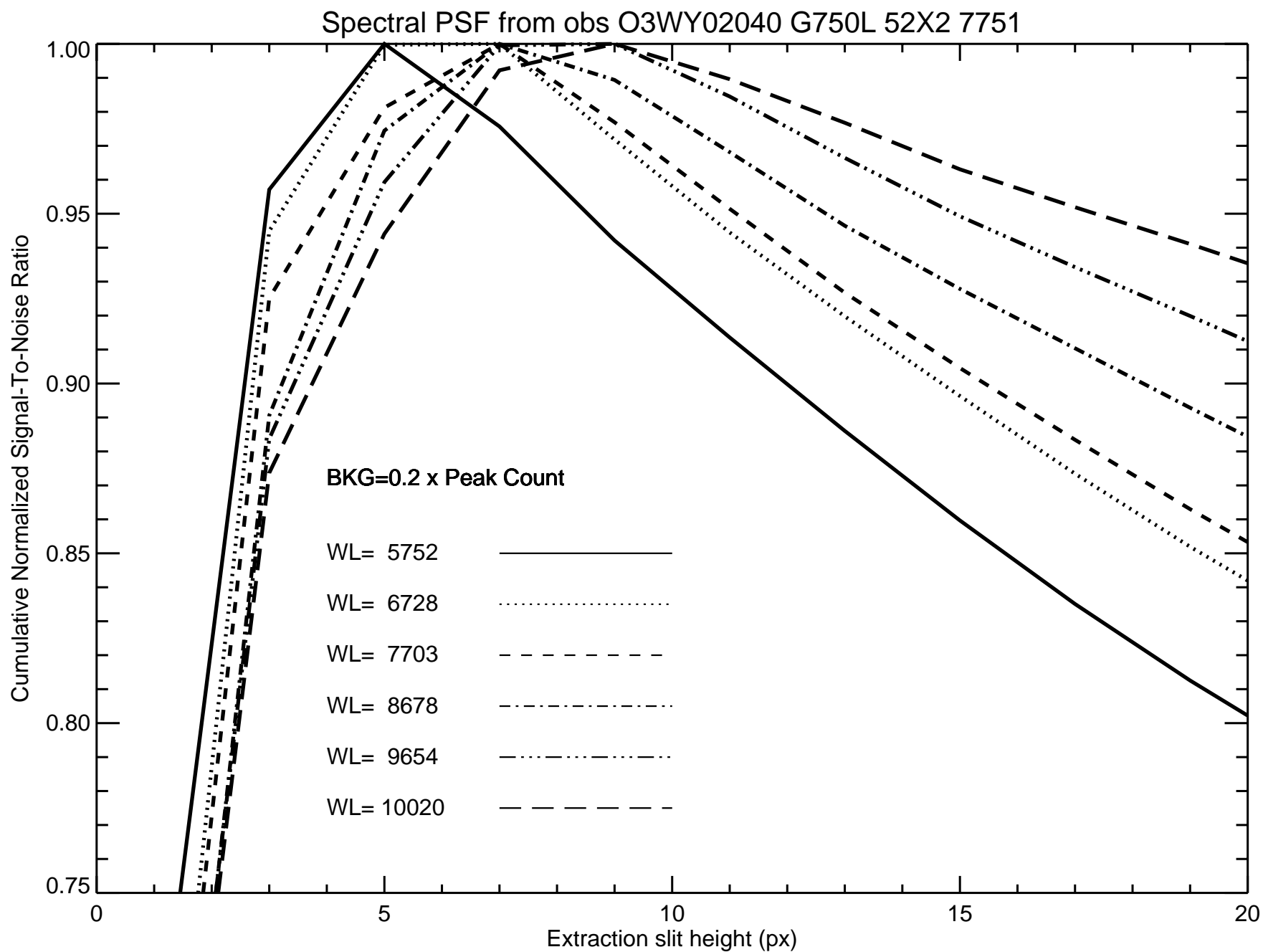


Fig. 4e

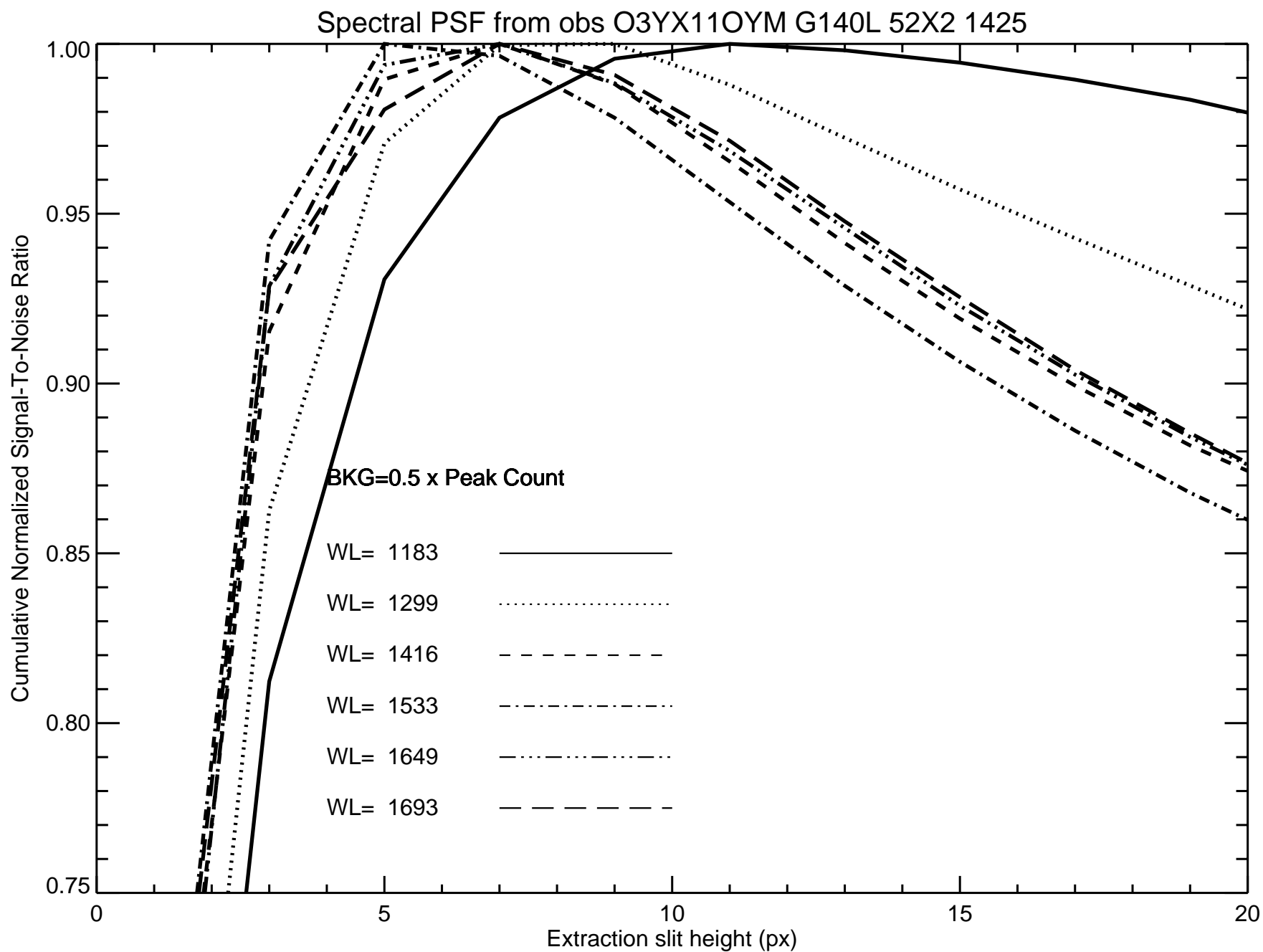


Fig. 5a

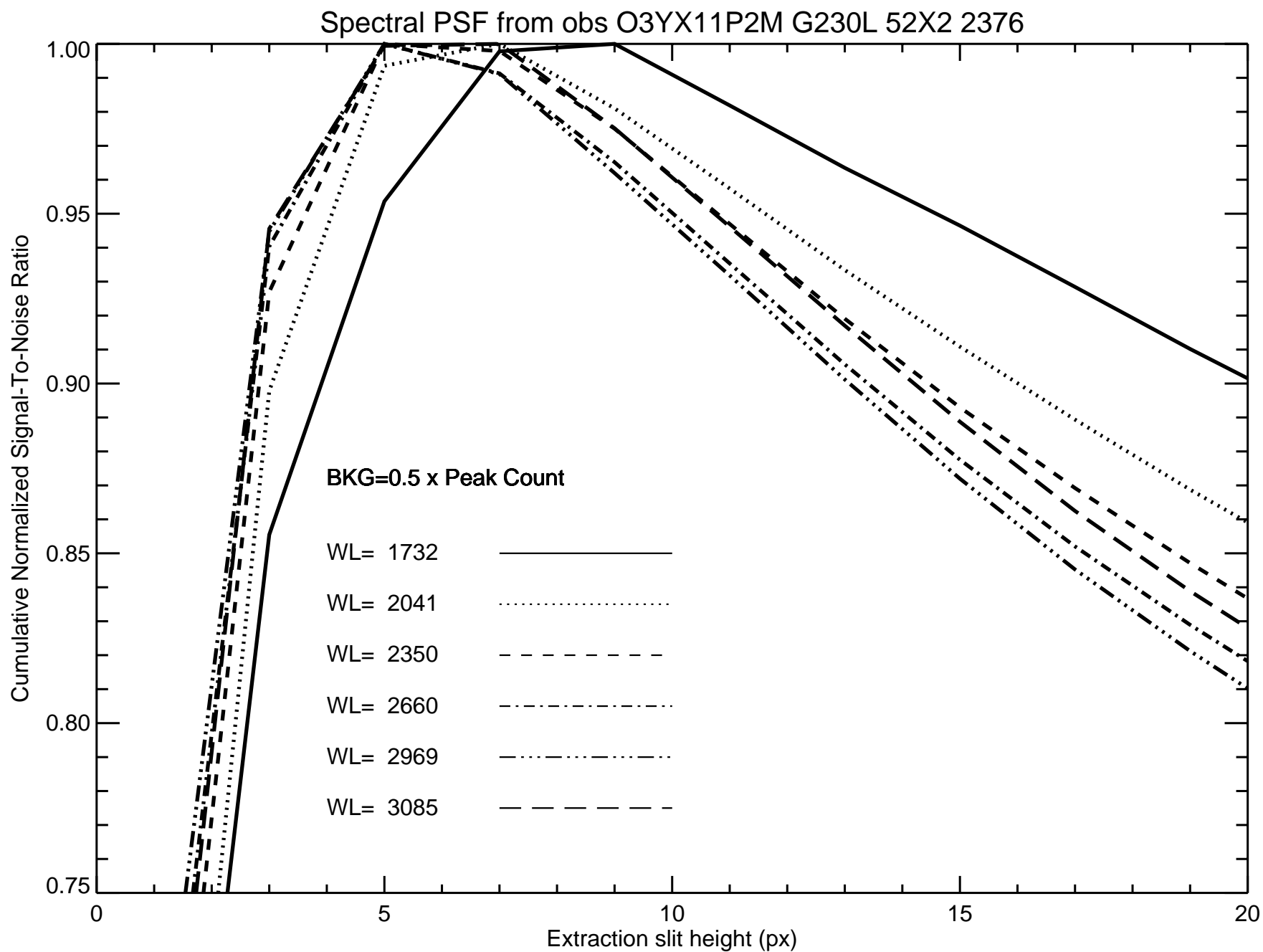


Fig. 5b

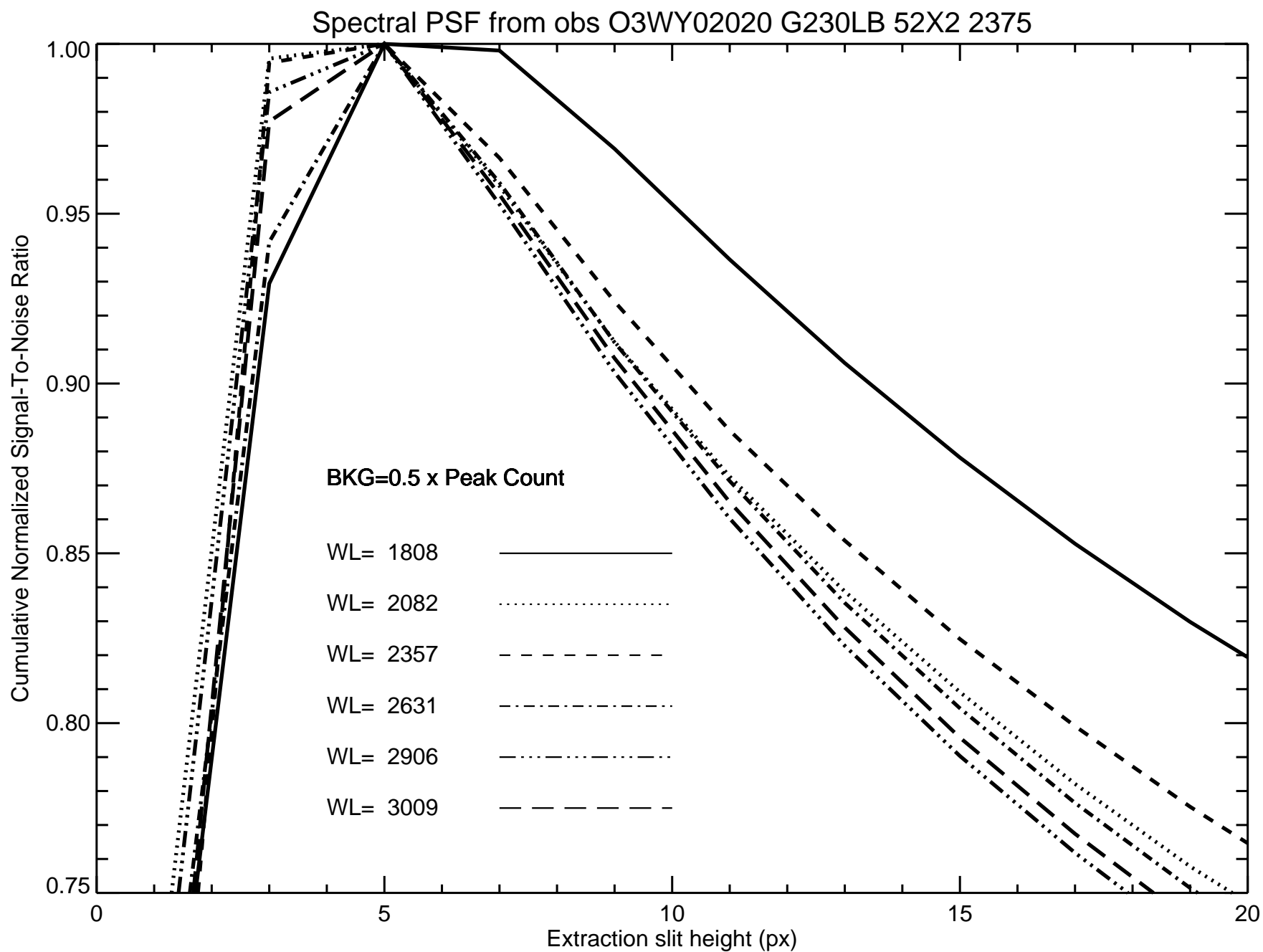


Fig. 5c

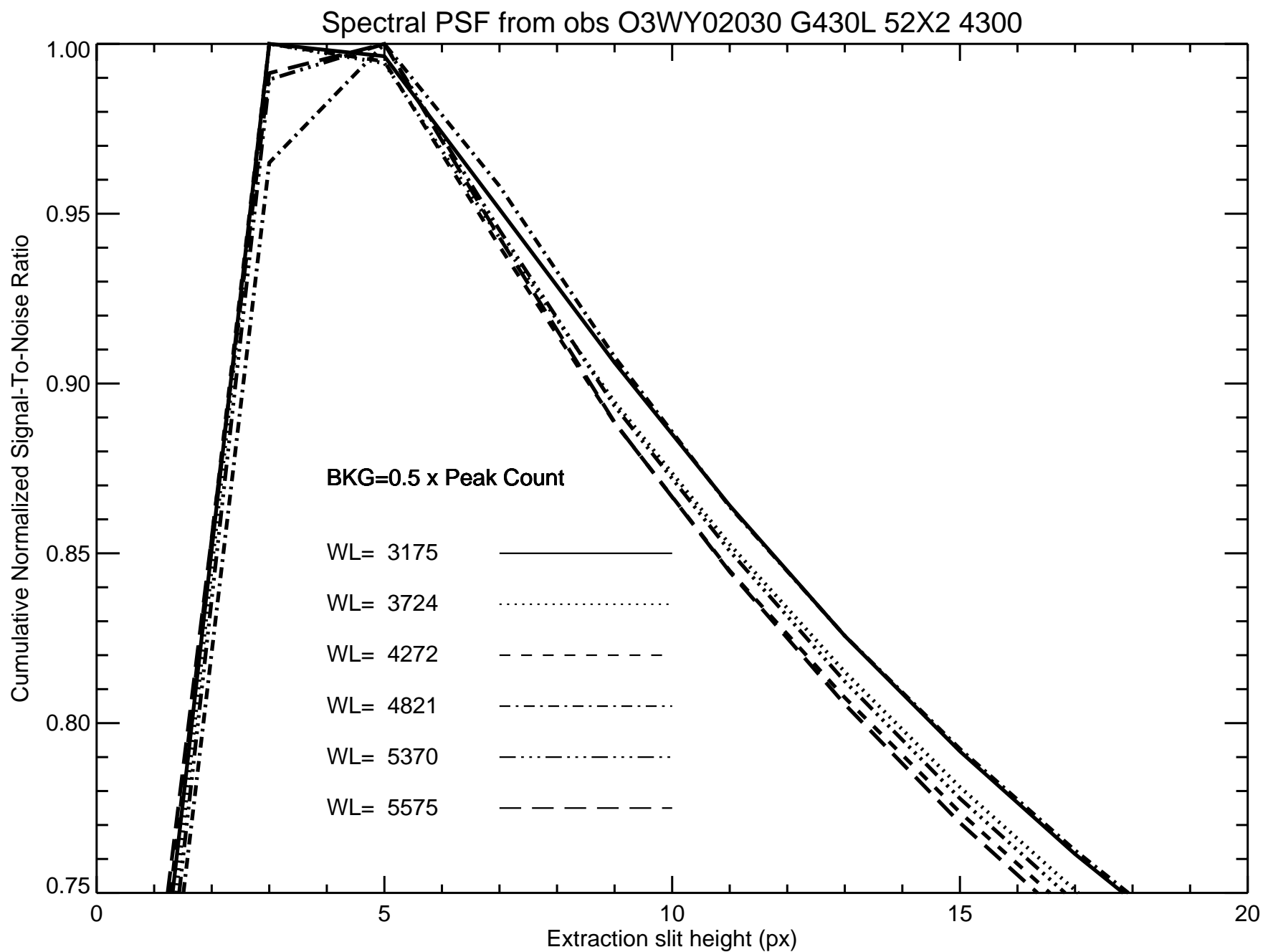


Fig. 5d

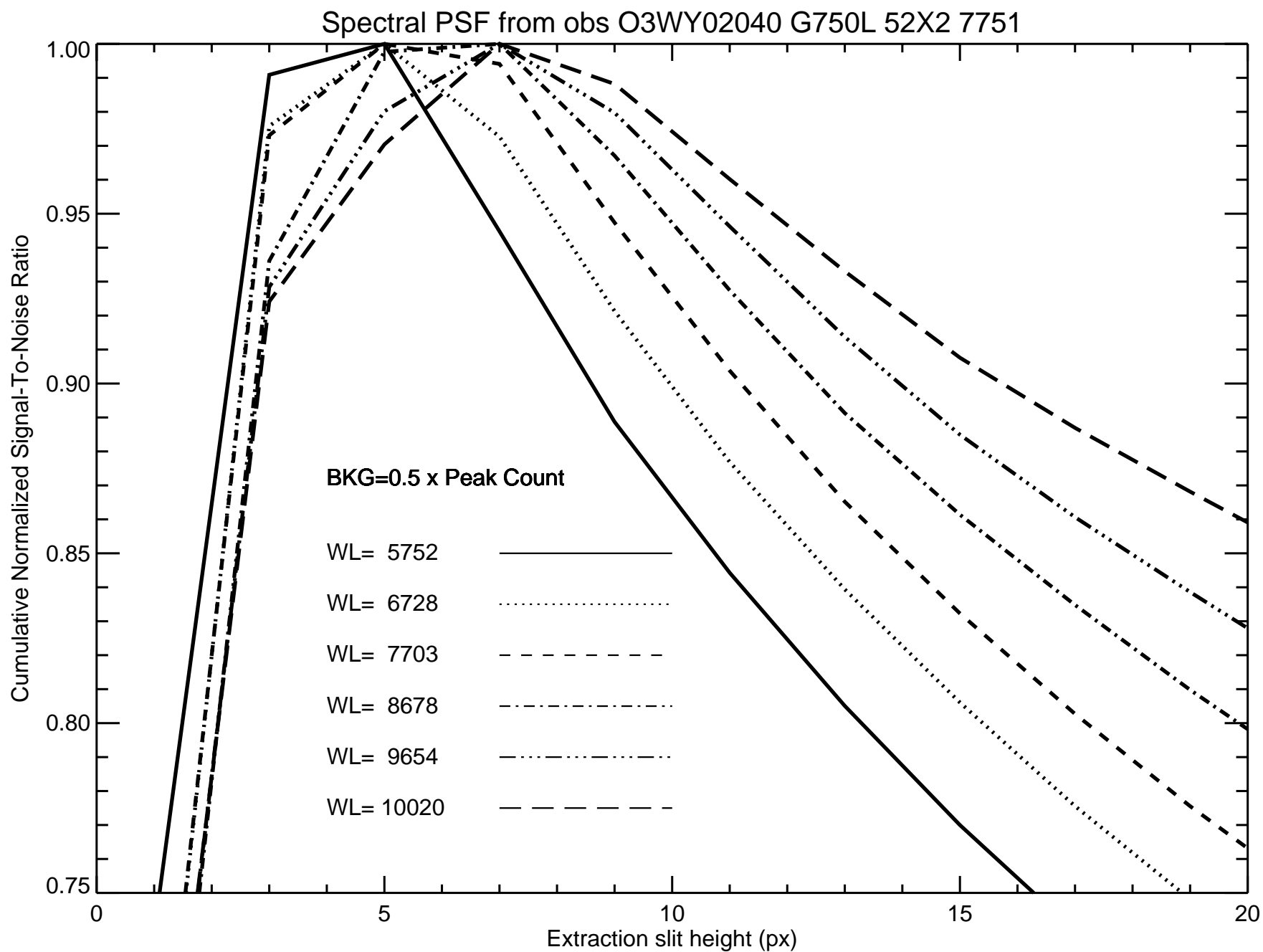


Fig. 5e

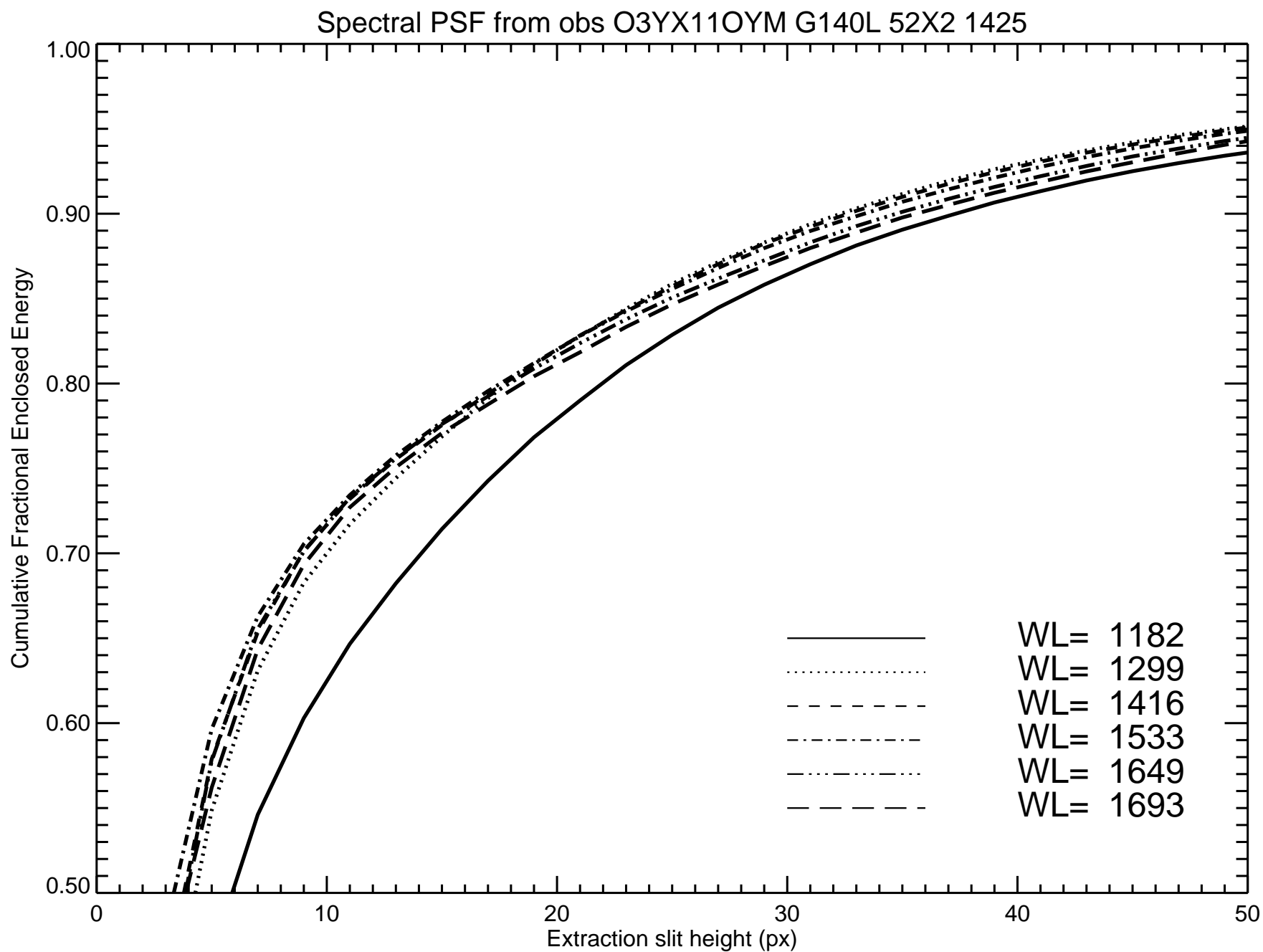


Fig. 6a

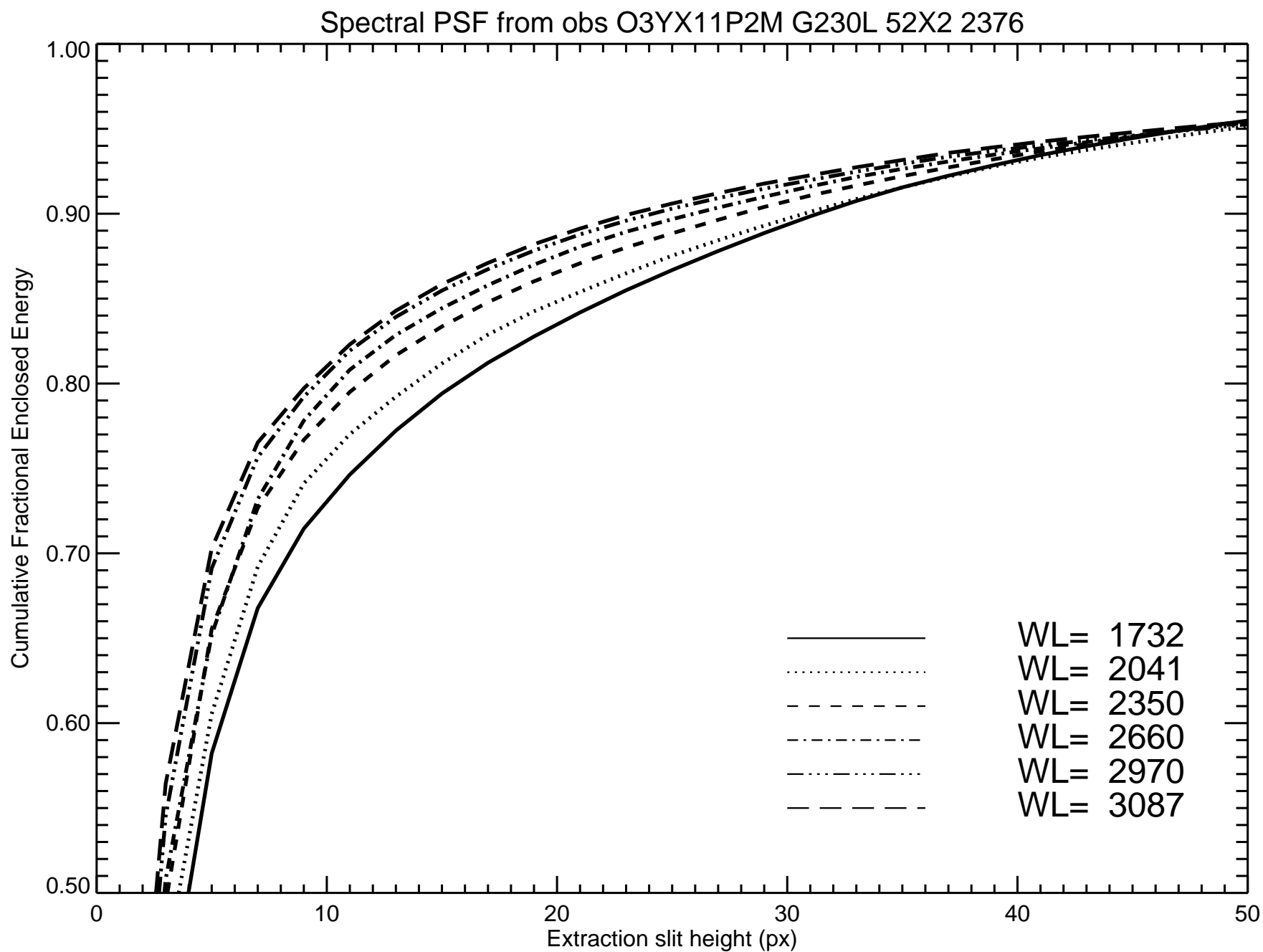


Fig. 6b

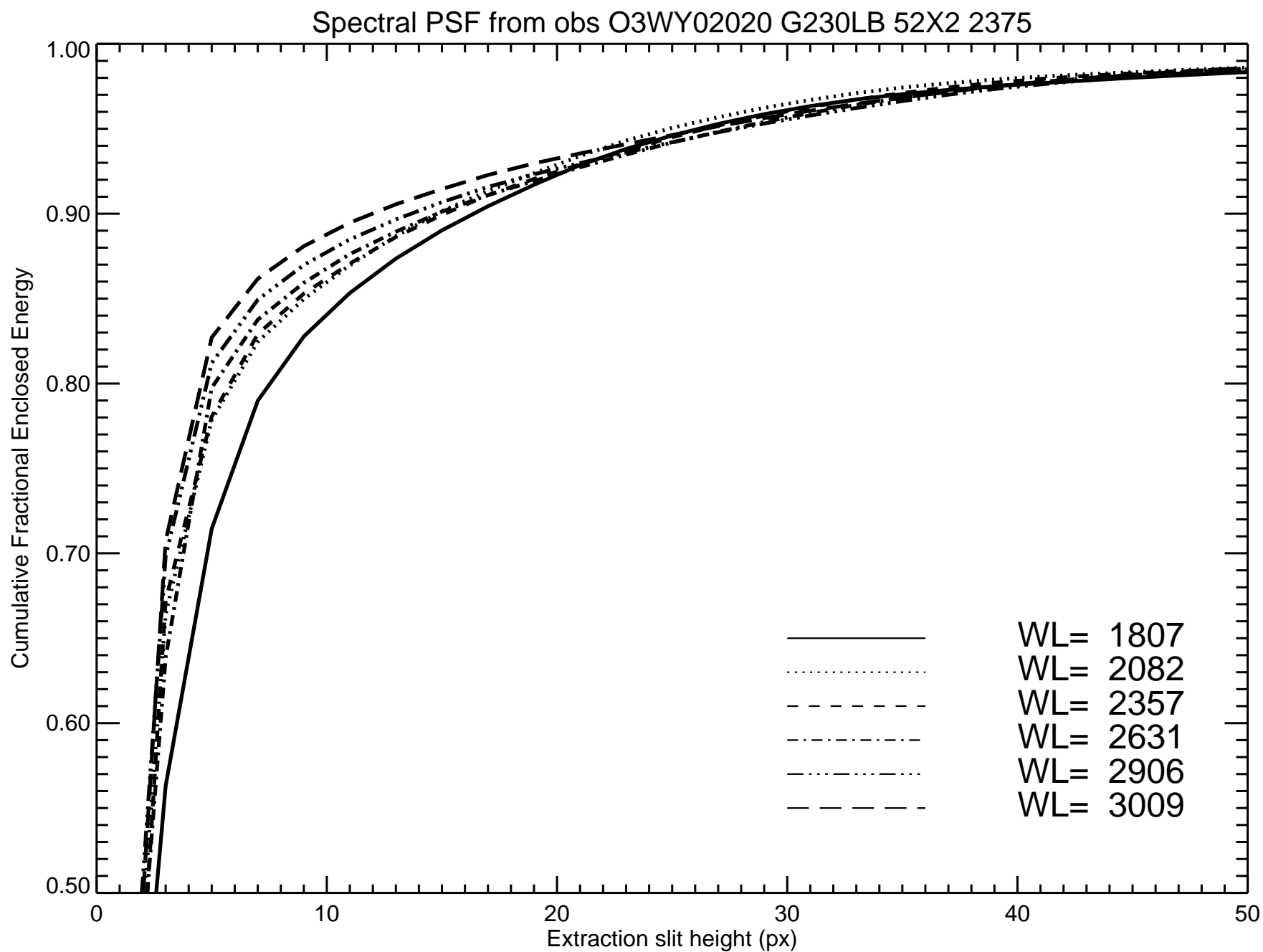


Fig. 6c

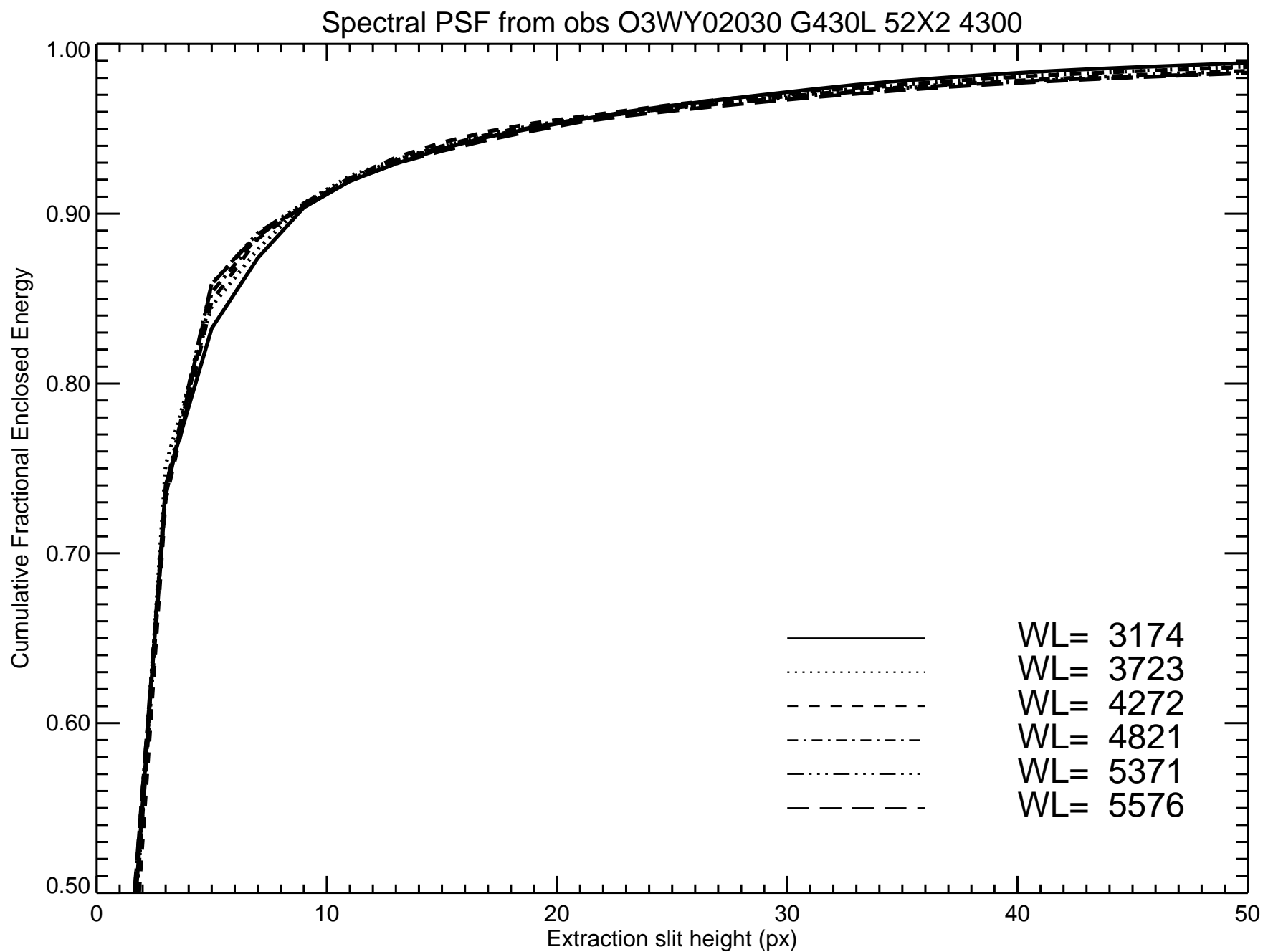


Fig. 6d

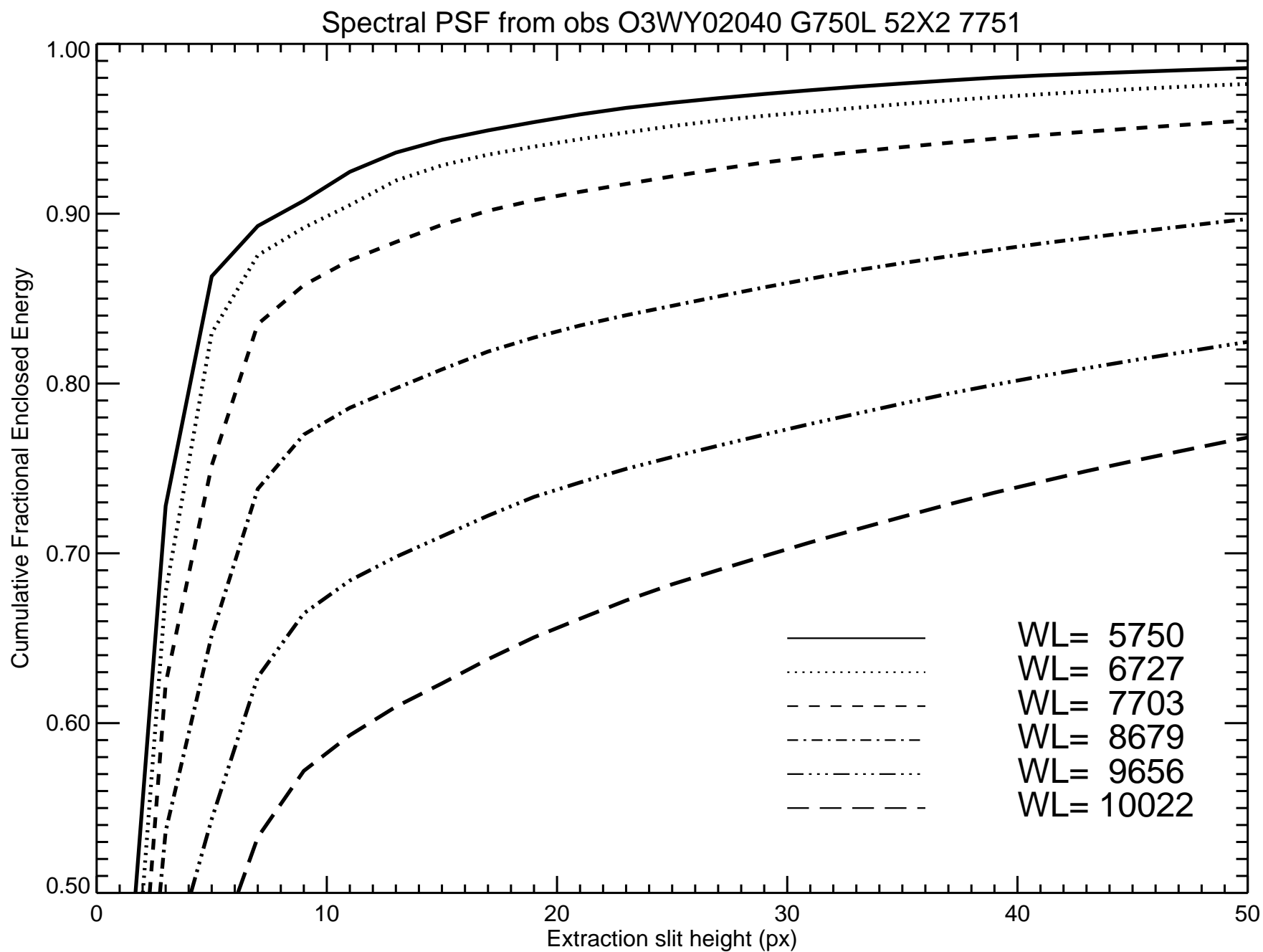


Fig. 6e

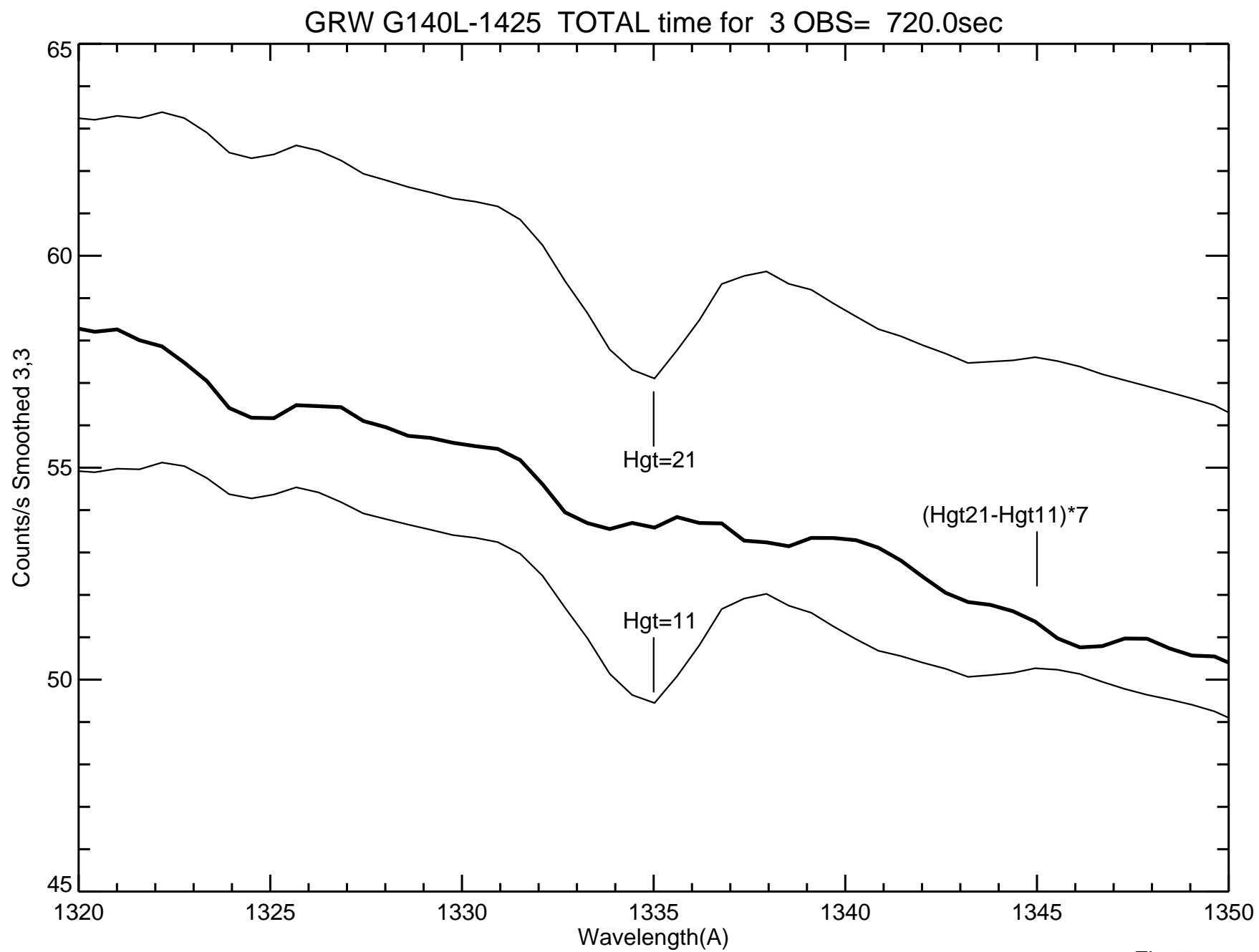


Fig. 7